Projections of an ice-free Arctic Ocean

Alexandra Jahn[1,2*], Marika M. Holland[3] and Jennifer E. Kay[1,4]

[1]Department of Atmospheric and Oceanic Sciences, University of Colorado Boulder, Boulder,CO,USA.
[2]Institute for Arctic and Alpine Research, University of Colorado Boulder, Boulder,CO,USA.
[3]Climate & Global Dynamics Laboratory, National Center for Atmospheric Research, Boulder,CO,USA.
[4]Cooperative Institute for Research in Environmental Sciences, University of Colorado Boulder, Boulder,CO,USA.

†Corresponding author(s). E-mail(s): alexandra.jahn@colorado.edu;

Abstract

Arctic sea ice loss is projected to continue in the future under all emission trajectories. In this Review, we assess the timing and regional variability of early ice-free and consistently ice-free conditions in the Arctic. Based on the current climate models, early ice-free conditions in the September monthly mean could occur in the 2020s or 2030s under all emission trajectories, and are likely to occur by mid-century. However, daily ice-free conditions in September could occur over a decade before monthly ice-free conditions, and on average occur 4 years earlier. Future emission trajectories will determine how often and for how long the Arctic could be ice-free. By 2100, there is potential for ice free conditions in May-January and August-October under a high and low emission scenario, respectively. Future research needs to prioritize refining predictions of ice-free conditions, including of regional ice-free conditions, while taking into account the irreducible uncertainty due to internal variability. Ideally this will include dedicated comparisons of different model selection, recalibration, and constraining methods, as currently too many things differ between studies to directly compare refinement methods for ice-free projection. Furthermore, more research is needed into both the impacts of an ice-free Arctic and the drivers of internal variability in Arctic sea ice that cause early ice-free conditions in models.

1 Introduction

The Arctic sea ice cover has declined rapidly in all seasons [1], including the sea ice area [G], sea ice extent [G] [2] and sea ice thickness [3, 4]. Areal summer sea ice loss in particular has been large, with a sea ice area [5] loss of -0.078 million km^2/year between 1979-2023. Spatial and temporal variability in areal sea ice cover loss is also evident [6], with a sea ice area loss of between 1996 and 2012 that was more than twice the average rate of ice loss over 1979-2023 (-0.17 million km^2/year versus -0.078 million km^2/year), and the largest sea ice concentration reductions seen in the shelf seas of the Arctic Ocean [6].

These losses in Arctic sea ice are considered among the earliest clearly attributable examples of anthropogenic climate change [7–9]. Indeed, climate models from the late 1970s predicted this decrease in sea ice cover in response to rising atmospheric greenhouse gases, including the possibility of reaching ice-free conditions during the summer with sufficient warming [10]. Given the observed and projected warming across the Arctic[11], which greatly exceeds the global warming (Arctic amplification), current climate models predict that an ice-free Arctic in September is likely before mid-century [12].

Complicating the accurate prediction of the likely timing of an ice-free Arctic, simulations have a large model spread [12], leading to ice-free timing differences that exceed 100 years [12, 13]. While part of this model spread can be explained by the approximately 20 year prediction uncertainty due to internal variability [14, 15], the majority of the model spread is due to physical differences between the models. To deal with the latter, the so called model or structural uncertainty, selecting, constraining or re-calibrating model projections has become common [12, 16–19]. However, the evolving definition of what exactly an 'ice-free' Arctic refers to complicates the understanding of predictions of an ice-free Arctic, as definition differences can lead to ice-free timing differences of several years to over a decade [15].

Regardless of prediction uncertainties, the predicted changes in the Arctic signify a regime shift from a perennial sea ice cover to a seasonal sea ice cover, or from a white summer Arctic to a blue Arctic [20] (Fig. 1) – a change that has likely not occurred for at least 80,000 years [21] (Box 1) – with important impacts on the local and global climate and ecological systems. For instance, the large reduction in albedo [G] when sea ice is replaced by open water modifies the radiation balance [22], accelerating and amplifying anthropogenic warming [23], especially in the Arctic [24–27]. Moreover, larger open water areas and longer periods of ice free conditions allow for larger fetch [G] [28], increasing wave heights [29, 30] and coastal erosion around the Arctic Ocean [31, 32]. From an ecosystem perspective, the transition towards a summer ice-free Arctic has negative impacts on sea ice dependent mammals such as polar bears and seals [33–35], while concurrently increasing ocean productivity [36] and allowing the potential migration of some fish species from the sub polar seas [37]. Economic activity in the Arctic could also increase owing to increased accessibility for shipping [38] and resource exploration [39].

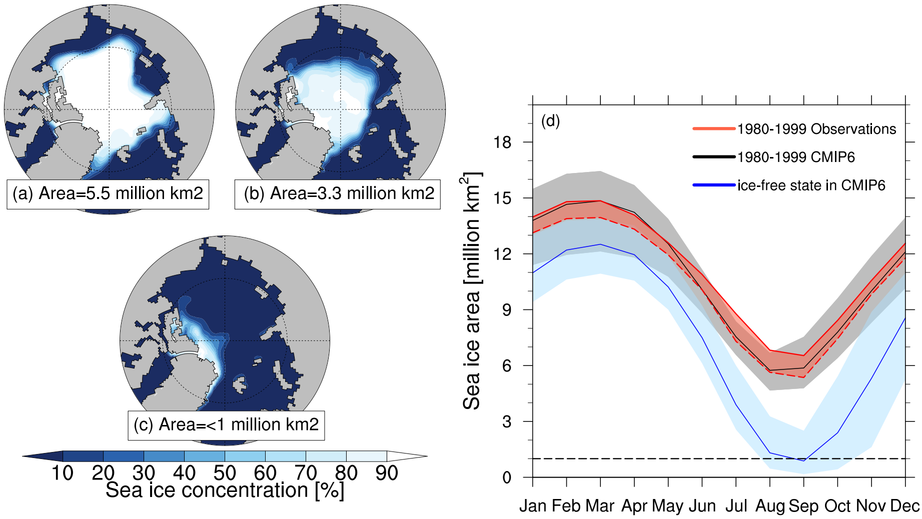

Fig. 1 White to Blue Arctic:.a, pan-Arctic [G] September sea ice concentration with a sea ice area of 5.5 million km^2, typical for the 1980s. **b**, as in a, but for 3.3 million km^2, typical for 2015-2022. **c**, as in a, but for sea ice area of <1 million km^2, referred to as an ice-free Arctic. **d**, the climatological seasonal cycle for 1980-1999 for satellite-derived sea ice area observations [40] (red) and from selected CMIP6 models [12] (black). The red shading indicates the uncertainty in the observed sea ice area, with sea ice concentration data using the bootstrap [41] (solid red line) and NASA Team [42] (dashed red line) algorithms. Grey shading indicates the CMIP6 ensemble spread. To show how the climatological seasonal cycle changes for an ice-free Arctic, the predicted seasonal cycle from the selected CMIP6 models is shown for a predicted ice-free September in the ensemble mean (blue), with light blue shading for the CMIP6 ensemble spread. While sea ice area is reduced in all months of the year in the future, the loss is predicted to be greatest in September, which also means that winter sea ice returns even after ice-free conditions are reached.

In this Review, we summarize the current understanding of projections for an ice-free Arctic. We begin by discussing the drivers of sea ice loss that lead to an ice-free Arctic, followed by a discussion of the various approaches and uncertainties to assess when the Arctic could become ice free. Next, we outline likely dates for an ice-free Arctic in September, months beside September, and regional ice-free conditions. Finally, we provide an outlook of future research needs. To illustrate the discussed approaches and ice-free projections, we analyze primarily monthly sea ice area from selected [12] CMIP6 [G] [43] models, supplemented by large ensemble simulations from both CMIP5 and CMIP6. The criteria for model CMIP6 selection used here is that observations fall within each models ensemble spread for two key metrics [12]: the 2005-2014 September mean sea-ice area, and the observed sensitivity [G] of sea ice area to cumulative CO_2 emissions over 1979-2014 (see Supplemental Table 1 for information on the models and specific ensemble members used).

2 Drivers of Arctic sea ice loss

Arctic sea ice changes are due to a multitude of interconnected processes. Among the processes affecting Arctic sea ice are changes in the heat transport into the Arctic in the atmosphere and the ocean (Fig. 2). These transports can vary due to internal climate variability as well as due to externally forced changes. Within the Arctic, feedbacks involving the sea ice cover itself [44] as well as local winds and ocean currents affect Arctic sea ice (Fig. 2). In the case of forced changes due anthropogenic greenhouse gas emissions, the fact that the majority of local feedbacks in the Arctic are positive leads to an amplification of Arctic sea ice loss and Arctic warming. Positive feedbacks [G] associated with declining sea ice, including the albedo feedback and lapse rate feedback, dominate in driving Arctic warming, but their magnitude is uncertain and varies across models [45, 46]. Negative feedbacks [G], such as the influence of ice thickness on ice growth rates [47], can mitigate ice loss somewhat but not enough to counteract declining trends. Notably, the strength of these feedbacks can be climate-state dependent [48, 49] and so their relative strength are expected to vary as sea ice changes.

The observed Arctic sea ice area loss is generally consistent with simulations from climate models, although the amount of the simulated ice loss varies considerably across different models [12], and to a smaller extent, across different ensemble members within a single model [15]. The range of simulated ice loss within single model large ensembles indicates large internal variability [G] is present even on multi-decadal timescales [8]. Indeed, through comparison of the inter-ensemble range of ice loss with the ensemble-mean change, large ensembles have been used to conclude that the observed loss of September sea ice is due to forced change from anthropogenic emissions that has been reinforced by internal variability [8]. Studies that isolate the role of atmospheric winds indicate that internal variability in atmospheric circulation may have reinforced the observed September ice loss by up to 50% [50, 51] and that atmospheric variability overall accounts for about 75% of Arctic sea ice internal variability [52]. Ocean heat fluxes into the Arctic, however, are also important for the variability in Arctic sea ice, and may have helped stabilize the September sea ice area between 2007-2023 [53].

Although internal variability has likely reinforced the observed summer Arctic ice loss, the magnitude of loss would not have been possible without anthropogenic greenhouse gas emissions [54] (Supplementary Fig. 1). Historical model simulations which apply subsets of external forcings (only natural forcings, only anthropogenic aerosol forcings, only greenhouse gas forcing) have enabled the attribution of forced changes in the climate. These show that greenhouse gas emissions drove considerable ice loss which was modestly offset by the cooling effects of anthropogenic aerosol emissions [55]. While CO_2 emissions were the most impactful for Arctic sea ice, other greenhouse gases have also contributed. For example, the radiative effects of chlorofluorocarbons have been found to account for about 48% of forced September sea ice loss from 1979-2005 [56]. Hence, the phasing out of these chemicals due to the Montreal

Protocol has delayed the occurrence of the first ice-free Arctic by about 10 years [57]. Thus, while observed sea ice loss has a roughly linear relationship with global mean surface temperature [58, 59] and with the cumulative carbon dioxide emissions [60], these relationships might not hold for the future given changes in the mix of external forcings that contribute to forced changes in regional Arctic warming and Arctic sea ice loss.

Textbook 1: The history of ice-free conditions in the Arctic

The Arctic Ocean was not always covered by sea ice. In the distant past (over 70 million years ago during the Cretaceous) early ancestors of tropical plants and crocodiles thrived in the Arctic [61–63]. Hence, ice-free conditions are not a first for the Arctic when assessed over the geological record. However, sea ice has been a defining feature of the Arctic Ocean for the last 47 million years [since the Eocene 21]. Perennial sea ice likely first appeared during the Miocene around 14-13 million years ago [64, 65], based on multiple lines of paleo evidence [see 21, 66, for detailed reviews of the reconstructed sea ice and climate of the Arctic]. After perennial sea ice first appeared, several periods of a return to seasonal sea ice have likely taken place [21, 67]. For example, paleo proxy evidence suggests that during the late Miocene (approximately 5 million years ago) ice free summer conditions re-occurred in the central Arctic Ocean [68], with several other periods of summer ice free conditions identified in the paleo record [21].

The last time ice-free conditions likely occurred in the Arctic was during the warmest period of the warmest interglacials during the Quaternary, the Eemian. Specifically, ice-free conditions occured during the so called Marine Isotope stage MIS 5e (between 130,000 and 115,000 years ago) as well as potentially also to the end of MIS5, MIS 5a (around 80,000 years ago). At these times, with paleo evidence stronger for the MIS 5e than for 5a, proxy records indicate open water north of Greenland [69–73] as well as a northward shift of the tree line by hundreds of km in Alaska and Russia [66, 74]. In contrast, during the current interglacial that started 11,000 years ago, the Holocene, the Arctic Ocean likely retained its perennial sea ice cover [67, 75]. However, there is evidence for regionally ice-free conditions in the Arctic during the mid Holocene warm period that peaked around 6000 years BP, in particular in the shelf seas of the eastern Arctic [21, 75, 76]. Thus, the perennial sea ice was likely much reduced in the summer during the mid-Holocene, and restricted to north of Greenland [75], where the oldest and thickest ice is found today [77, 78].

Thus, when pan-Arctic ice-free conditions occur again in the next few decades, it will likely be a first for at least 80,000 years [70, 71], if not for over 115,000 years [73]. The occurrence of pan-Arctic winter ice-free conditions, predicted to occur in the 23rd century under extreme warming [79], would be a first for 47 million years, since the Arctic became sea ice covered in the Eocene. [21].

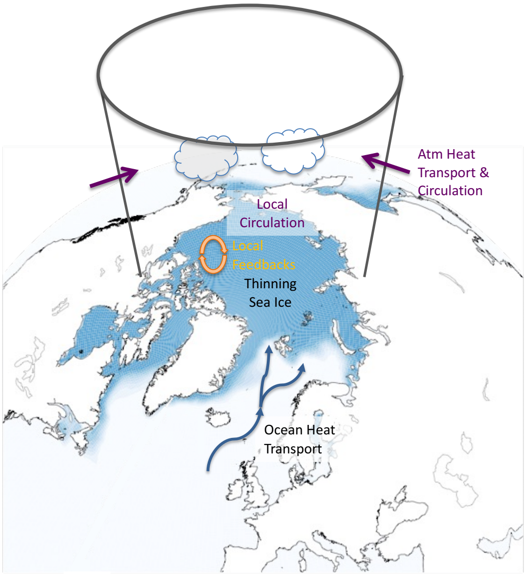

Fig. 2 Schematic of processes driving Arctic sea ice loss. Processes that drive Arctic sea ice melt in response to large-scale changes in the radiative forcing are themselves affected by the Arctic sea ice loss, illustrating that the climate system is highly coupled.

The preponderance of positive feedbacks in the Arctic have led some to posit that a tipping point [G] might exist with regards to sea ice loss [80]. Simple climate models did show evidence of a tipping point in Arctic sea ice [81, 82]. However, more complicated systems show no indication that a sea ice tipping point exists [83–85]. This lack of a tipping point in Arctic sea ice was found to be due to the stabilizing influence of the annual cycle of solar insolation and meridional heat transport as included in more complex modeling systems [86]. Hence, if climate forcing such as increased CO_2 is removed in complex climate models, the sea ice recovers within several years as temperatures decrease [83–85].

The combined influence of anthropogenic forcing, strong positive feedbacks, and substantial internal variability has the potential to lead to large multi-year changes in the Arctic sea ice, commonly referred to as Rapid Ice Loss Events (RILEs) [87]. As Arctic sea ice thins, large areas of the ice pack are susceptible to melt out, resulting in increased summer ice area variability [88, 89] and a higher likelihood of RILEs. These RILE events are influenced by ocean heat transport variations [87, 90], atmospheric circulation anomalies [91], or a combination of the two [92]. The surface albedo feedback and fall cloud feedbacks reinforce these events [93]. Notably, periods of limited ice loss are also possible when internal variability counteracts anthropogenically forced change [8]. The evolution of these high and low ice loss events affects the trajectory by which summer ice free conditions are reached within the Arctic, and allow for the possibility of reaching ice-free conditions within a few years when starting from the average sea ice cover in the early 2020s.

3 Methods for the prediction of an ice-free Arctic

Predictions of an ice-free Arctic can be based on different definitions, as well as using different methods, each with their own inherent uncertainties. Hence, to better understand existing predictions of an ice free Arctic (Table 1), the different definitions and methods used for their predictions are now discussed. This will be followed by a discussion of the different kinds of uncertainties important for ice-free predictions.

3.1 Different definitions of an ice-free Arctic

The exact definitions of what an "ice-free Arctic" refers to has varied. Early on, it was usually defined as the nearly complete disappearance of all sea ice, as measured by zero sea ice extent [10, 87, 94]. As the thickest sea ice north of Greenland and the Canadian Arctic Archipelago remains for over a decade after the rest of the Arctic Ocean is free of sea ice in September [87, 95], it became common to use a sea ice extent threshold of 1 million km^2 to refer to ice-free conditions [54].

When the 1 million km^2 threshold is used for sea ice area rather than ice extent [12, 60, 96], an ice-free Arctic occurs earlier than using sea ice extent [97] (Fig. 3a). Specifically, for the selected CMIP6 models [12], using sea ice area rather than extent leads to ice free conditions between 0 and 47 years earlier, with a mean of 8 years, a mode of 3, and a standard deviation of 10 years. Note also that while sea ice area is commonly defined as the sea ice concentration times the grid area, sometimes sea ice area calculations used for projections additionally used a minimum threshold of 15% sea ice concentration [17, 98], which leads to even earlier ice-free dates than using sea ice area.

Ice-free conditions have also been based on smoothed timeseries or ensemble means of the sea ice cover [13, 16, 99] or have used the unsmoothed monthly sea ice data[15, 54, 100–103]. This diversity of definitions of ice-free conditions causes challenges in comparing existing ice-free predictions (Table 1), as definition differences of an ice-free Arctic can affect the timing of ice-free conditions, ranging from a few years to well over a decade (Fig. 3a).

When assessing what predictions are actually predicting by using different definitions of an ice-free Arctic, two clear categories emerge: predictions of the "earliest ice-free conditions", obtained using monthly sea ice timeseries with a large influence of internal variability. And predictions of ice-free conditions due to the forced response, based on smoothed data, which will be referred to here as "consistently ice-free conditions".

The category of "consistently ice-free conditions" it not a homogeneous category, but includes a variety of different definitions. This category is chosen to separate predictions of the earliest possible ice-free Arctic, which could be a single occurrence caused by internal variability once the mean sea ice state is low enough, from approaches focused on detecting ice-free conditions based on the forced response. Thus, consistently ice-free conditions represent the time after which ice-free conditions are likely to occur in a given year. Methods used to calculate consistently ice-free conditions include using timeseries smoothed by 5+yr running means [58, 94, 104, 105], using ensemble means [96], the use of 5 consecutive ice-free years [13, 15, 101, 106], or "likely" ice free conditions based on cumulative probabilities [18, 107]. Through all of these methods, the predicted occurrence of first ice-free conditions is delayed (Fig. 3a) compared to using unsmoothed monthly data, shifting the focus to the likely occurrence of ice-free conditions based on the forced response rather than the earliest possible occurrence of ice-free conditions.

The difference between earliest ice-free dates and consistently ice-free dates varies based on the strength of the forcing applied: The stronger the forcing, the closer the time of a possible first ice-free Arctic will be to the time of consistently ice-free conditions (Fig 3a). For example, while the difference between predictions of first ice-free conditions and consistently ice-free conditions are only a few years for SSP5-8.5, it is around 15 years for SSP1-2.6 (Fig 3a).

When predictions of an ice-free Arctic are given in terms of cumulative probabilities [101, 103, 107, 108], one can infer both the occurrence of the first possible ice-free Arctic (any % above 0) and of consistently ice-free conditions. For the latter, there are different thresholds that one could use to define a consistently ice-free conditions. Based on the mean of other definitions for forced ice-free conditions, consistently ice-free conditions correspond to the start of the "likely" cumulative probability, at >66% (Fig. 3a versus c). Due to the ability to provide predictions of both categories of ice-free conditions, cumulative probabilities are therefore a useful way to display predictions of first ice-free conditions in a comprehensive manner.

3.2 Different prediction methods

The most common ice-free predictions for the Arctic have been made based on projections from climate models [10, 12, 17–19, 54, 57, 94, 97, 98, 100, 101, 103, 109, 110]. Climate models explicitly simulate the evolution of sea ice, including dynamical and thermodynamical processes, albeit always in an incomplete way due to limitations on our understanding of the climate system and computational constraints. Climate models can provide both predictions of early and consistently ice-free conditions, based on how the mode output is analyzed.

Statistical methods have also been used to provide predictions of an ice-free Arctic. These include projections based on the observed linear relationship between global temperature or CO_2 and sea ice cover [1, 58, 111, 112], and the use of more complex statistical models [107, 113]. Note that these statistical methods typically assume that observed relationships will continue into the future, which may or may not be accurate. Furthermore, as statistical method usually rely on linear relationships that represent that response of sea ice to forcing, they lead to predictions of consistently ice-free conditions. In order to also provide early ice-free predictions, some statistical ice-free predictions have included a statistical representation of internal variability [107, 111, 112]. As the statistically added internal variability is usually based on standard deviations from observations or models, the kinds of rare sea ice loss events, such as RILEs or single year events like 2012, that are including depends strongly on how the internal variability is estimated. Using $\pm 3\sigma$ [107] accounts for 99.7% of the internal variability, and hence only truly rare events (0.3%) are not accounted for. However, if $\pm 1\sigma$ [111] or $\pm 2\sigma$ [112] are used to add internal variability to statistical predictions, this means that 32% or 5% of the full internal variability range is not captured, likely delaying the prediction of early ice-free conditions.

3.3 Inherent uncertainties of predictions

For predictions of any kind to be useful, it is paramount to understand the limits of predictability, so as not to confuse precision with accuracy. For climate model predictions, the prediction uncertainty is due to three main causes: Internal variability uncertainty, model uncertainty, and scenario uncertainty [114]. For statsitical methods, the prediction uncertainty is due to four main causes: Observational uncertainties [111], uncertainties in the observed relationships, scenario uncertainty and internal variability uncertainty (or neglecting internal variability uncertainty).

Internal variability prediction uncertainty is caused by the chaotic nature of the climate system [115] and as such is irreducible. Hence, even with improvements in models and/or methodology, predictions of the ice-free Arctic will always have an internal variability uncertainty range. The magnitude of this internal variability uncertainty for predictions of a first ice-free Arctic is around 20 years [14, 15], but can be even larger for some models [116] (Supplementary Fig. 2). For consistently ice-free conditions, the internal variability uncertainty range is usually slightly reduced (Supplementary Fig. 2), as some internal variability is averaged out. The only way to possibly reduce but not eliminate internal variability uncertainty is related to understanding the underlying drivers of the internal variability, and refining predictions based on the potential predictability of those drivers [117]. Furthermore, as the time of an ice-free Arctic comes closer, initial-value predictability [G] of sea ice might allow for more precise predictions, but this predictability is limited to seasonal to interannual timescales [118].

Scenario uncertainty is due to the uncertainty about the evolution of net future emissions of greenhouse gases, from all sectors including land use. As such, it is an uncertainty that is not reducible as it depends on the future decisions of societies and policy makers. To provide predictions that do not depend on the specific emission scenario used, predictions of an ice-free Arctic can be provided in terms of degrees of global warming [12, 58, 59, 103, 112] (Fig. 3d) or cumulative CO_2 emissions [12, 60] instead of time.

Observational uncertainties in regards to the large-scale sea ice products used for projections of ice-free conditions relate to the uncertainties introduced through the remote sensing techniques compared to the actual sea ice conditions being observed. Depending on the methodology used to retrieve information about Arctic sea ice, the source of these uncertainties can be due to atmospheric interference, algorithmic uncertainties, and the spatial resolution of sensors [119]. One way to quantify the magnitude of observational uncertainty is to compare different products [12, 111, 119] (Fig. 1d).

Uncertainties in the observed relationships can be due to short timeseries [120] and/or due to uncertainty in whether historical relationships on which predictions are based will continue into the future. An example of the challenges associated with using short observational timeseries for predictions is the use of the linear trend in the observed sea ice volume over 12 years (1996–2007), which when extrapolated into the future led to a prediction of the earliest possible ice-free Arctic in 2016±3 years [121]. This prediction was not realized because the observed rate of sea ice decline is not constant in time. This example illustrates why linear extrapolation, especially of short timeseries, is not a reliable prediction method.

Model uncertainty is due to the structural differences in climate models, that is the different choices that are made in building individual climate model components. The structural uncertainty is the largest source of uncertainty for predictions of an ice-free Arctic and sea ice projections in general [12, 13, 122]. It is also the source of uncertainty that has the largest potential for reductions, as models are improved in the future and as methods to re-calibrate and constrain model projections are being developed. For the timing of ice-free conditions, the prediction range due to model uncertainty in non-refined projections is over a hundred years [12, 13] (Fig. 3b). Noteably, this large multi-model spread has persisted for close to two decades [12], despite improvements in sea ice model physics over that time. The persistence of the large model spread in sea ice simulations illustrates that while there is potential to reduce the model uncertainty by improving climate models, improving model physics does not always yield immediate improvements in predictions.

Efforts to reduce the large multi-model spread in projections of an ice-free Arctic have used model selection [12, 13, 16, 17, 54, 100, 123], model weighting [96, 122, 124], emergent constraints [98, 105], and model recalibration or constrained estimation [18, 19, 59]. For all of these, there currently is no one established set of metrics to use, as no consensus exists yet on which metrics have the most important impact on the future evolution of Arctic sea ice [13, 59].

For model selection or weighting, primarily sea ice variables such as the mean sea ice area or extent, the climatological seasonal cycle of sea ice area or extent, and sea ice trends have been used, together with rates of warming or cumulative CO_2 emissions [12, 13, 54, 122]. However, using April sea

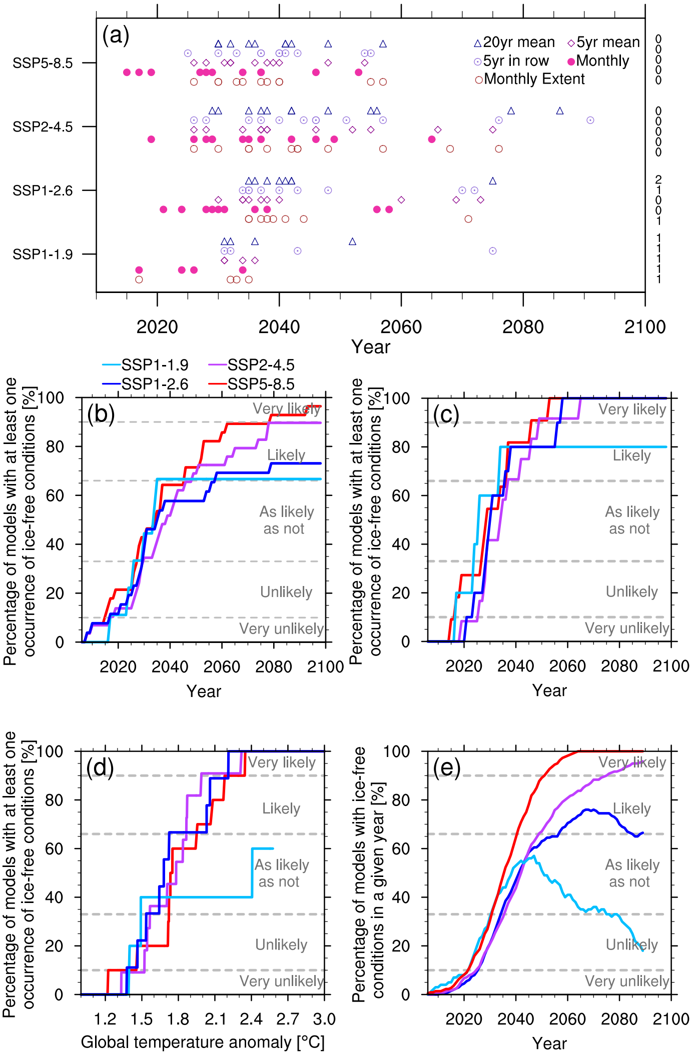

Fig. 3 Influence of different ice-free definitions and model selection on the timing of the prediction of an ice-free Arctic. a, year of the earliest ice-free conditions in September for different definitions in the 'selected CMIP6 models' (selection based on their performance over the historical period [12], see Supplementary Table 1). "Early ice-free conditions" use unsmoothed monthly sea ice area (same method as used in b–e) or monthly sea ice extent data; "consistently ice free conditions" refers to definitions using 5yr smoothed sea ice area, using 20yr smoothed sea ice area, or using the unsmoothed sea ice area but looking at the first year after which the Arctic is ice-free for 5 years. The numbers on the right y axis indicate the number of models that do not go ice-free by 2100 for a given model, definition, or scenario. **b** the fraction of CMIP6 models that have reached ice-free conditions at least once in the monthly mean September sea ice area by a given year under a given SSP [G] forcing scenario – the cumulative probability of first ice-free conditions – and their likelihood according to IPCC definitions. **c**, as in b, but for the selected CMIP6 models also shown in a. **d**, as in c, but showing the fraction of selected CMIP6 models that are ice-free for a given temperature anomaly (using a 5 year smoothed mean to reflect the level of forced warming rather than individual year temperatures), with the anomaly calculated relative to each models 1850–1899 global temperature. **e**, as in c, but showing the fraction of selected CMIP6 models that are ice-free in a given year, smoothed by a 20yr running mean.

ice thickness and its relation to summer sea ice area has been shown to narrow the CMIP6 projection uncertainty of an ice-free Arctic more than any of previously used sea-ice based metrics [17]. Hence, sea ice thickness should be considered as a commonly used metric to select models. Furthermore, using the northward ocean heat flux as model selection parameter moved the prediction of ice-free conditions 10 years earlier compared to using only sea ice based parameters [16]. The transition to an ice-free Arctic can also be affected by the Arctic Ocean hydrography, in particular the stratification of the upper Arctic Ocean [125]. Given the biases in the CMIP6 model's in regards to the Arctic stratification [126, 127] and the properties of the underlying warm Atlantic water [126, 128], the importance of including oceanic variables in the model weighting and selection should be further assessed.

Complicating the understanding of ice-free predictions, different refinement methods appear to lead to differences in the projected timing of ice-free conditions. Different recalibration methods influence the projected timing of ice-free conditions, as demonstrated by earlier ice-free dates when scaling the simulated SIA response to greenhouse gas forcing [18], whereas a recalibration of the SIE sensitivity to atmospheric circulation leads to later ice-free dates [19]. However, due to differences in the underlying data and the definitions of ice-free, as well as different numbers of CMIP6 models used, it is currently not clear what the pure effect of the different recalibration methods is.

The inability to compare the effect of different model selection or refinement methods on ice-free projections directly, due to differences in the underlying data and the definition of ice-free condition's used, highlights the need for dedicated inter-comparison studies to assess the different proposed model selection and recalibration methods. Such an effort has the potential to advance the field, by creating a common set of metrics to use to select and/or refine sea ice projections, as well as establish a common ice-free definition to use going forward.

4 Predictions of an ice-free Arctic

Taking into account the discussed prediction uncertainties and definition differences, the following section will discuss pan-Arctic ice-free predictions for September, ice-free conditions for months outside of September, and regional ice-free conditions.

4.1 Pan-Arctic predictions for September

Current predictions using a variety of models and methods suggest that an early first ice-free Arctic could occur potentially in the 2020s to 2030s, and is likely to have occurred by 2050 [12] (second column in Table 1 and Fig. 3c). In terms of temperature, early ice-free conditions could occur for any warming above 1.3 °C and are likely to occur for global warming of 1.8 °C above pre-industrial temperatures (Fig. 3d and Table 1). However, there is a large range of early ice-free predictions, ranging from the 2010s to past 2100 [12, 13] and 0.9–3.2 °C [12] (Table 1). Refined projections, through model selection, weighting, adjusting, and constraining, reduce the projections of early ice-free conditions to 2015 to the 2050s or 1.3–2.9 °C for the CMIP5 and CMIP6 models ([12, 18, 96, 100]). Which refined projection is the most accurate is an important open research question. It can currently not be answered, as too many variables differ between different existing refined ice-free predictions (as discussed in detail at the end of the previous section).

There is no influence of future emission scenarios on these predictions of early first ice-free conditions (Fig. 3c and d)[12, 96, 97], due to the short lead-time and the resulting small difference between the trajectories till then [129, 130]. Thus, the occurrence of an early first ice-free Arctic will be determined by internal climate variability [15], once the sea ice has retreated enough that ice-free conditions can be reached within the range of internal variability. For example, conditions similar to those that caused the observed record minimum Arctic sea ice cover in September in 2007 [131] and 2012 [132] could lead to the drop of sea ice below the 1 million km^2 threshold once the mean sea ice area is around 2 million km^2 or less. Early ice-free conditions could also be the result of a multi-year RILE [87, 90]. Such large single-year or multi-year ice-loss events could lead to ice-free conditions considerably earlier than when consistently ice-free conditions are expected [15]. However, as noted earlier, internal variability can both enhance the forced response or oppose it [8]. Hence, internal variability could also delay the occurrence of the first ice-free Arctic, so that the first ice-free Arctic potentially occurs later than when consistently ice-free conditions are expected [15].

Despite no impact of emission scenarios on the timing of an early first ice-free Arctic, there remains a small ($<$10%) yet non-zero chance to avoid ice-free conditions all together if warming is limited to below 1.5 °C [101–103, 108, 111, 133] (Fig. 3d), or only exceed 1.5 °C for a short period of time. The latter is the case in SSP1-1.9, where the multi-model mean global temperature anomaly stays below 2 °C and decreases again after mid-century [134], with not all models reaching any ice-free conditions (Fig. 3b, c, d).

How frequently ice-free conditions re-occur after a first ice-free September, however, depends very strongly on the future emission scenarios and the associated global warming [101, 103] (Fig. 3e). If ice-free conditions do occur for warming of 1.5 °C or less, they would likely not re-occur for several decades [101, 133]. For global warming of 2 °C , however, ice-free conditions in September would likely re-occur every two to three years after a first ice-free Arctic [101, 103, 133]. And for warming above 3 °C , they would occur again almost every year in September [101, 103], comparable to what is seen for the selected CMIP6 models under the SSP2-4.5 and SSP5-8.5 scenarios (Fig. 3e). Notably, if temperatures decrease again, probabilities of ice-free conditions in a given year will also decrease, as can be seen for SSP1-1.9 (Fig. 3e).

Consistently ice-free conditions are expected by mid century (column two in Table 1). In terms of warming, consistently ice-free conditions begin to occur for warming of 1.8 °C or more based on the literature (see column two in Table 1). The projection uncertainty for consistently ice-free conditions is lower than for early ice-free conditions, as the influence of internal variability on averaged is reduced (Supplementary Fig. 2). Nonetheless, predictions range between 2023 and 2085 (Table 1), with refined projections from CMIP5 and CMIP6 models showing consistently ice-free conditions between 2035–2067. As for the early ice-free conditions, comparisons of the different refinement methods are needed to understand the exact impact of different projection refinement methods.

The occurrence of consistently ice-free conditions signifies the transition to a new regime in the Arctic, where the Arctic is typically no longer covered by sea ice year-around and instead is frequently seasonally ice-covered. Hence, in terms of impacts, the transition to a consistently ice-free state is arguably the more meaningful date compared to early ice-free conditions. Nonetheless, early ice-free conditions will receive large attention if and when they occur, and hence the possibility of their occurrence and their predicted timing are important to determine and communicate.

All previous predictions of ice-free conditions used monthly means. Yet, the very first time the sea ice area dips below the 1 million km^2 ice-free threshold will be detected in the daily satellite observations. Based on calculations from the CESM2-LE [135], a large ensemble with a CMIP6 model, the first occurrence of daily ice-free conditions happens on average 4 years before the September monthly mean is first below 1 million km^2 (Supplementary Fig. 3), with a range of 0–18 years. In 56% of the CESM2-LE members the daily ice-free conditions occur earlier than the monthly ice-free conditions (Supplementary Fig. 3b), while for 44% of the CESM2-LE members, daily and monthly ice-free conditions first occur during the same year. Differences of 10 years or more thereby occur in 20% of the CESM2-LE members, with the largest differences occurring for ensemble members that have relatively late monthly-mean ice-free conditions (Supplementary 3b). Hence, it is important to note that ice-free conditions in the daily observations could occur even earlier than the likely dates for an ice-free Arctic based on the monthly analysis of the CMIP6 models, and hence even earlier than in the 2030s or 2040s (Fig. 3c). Note that these predictions are based on sea ice area, which leads to earlier ice-free dates than using sea ice extent (Fig. 3a).

4.2 Seasonality of reaching ice free conditions

Ice-free conditions in the Arctic can occur not just in September, but given a large enough warming, also for other months of the year [1, 101, 111, 112]. Generally, the larger the warming, the more months can be ice-free, expanding around September (Fig. 4). Ultimately, that means that the Arctic can also become ice-free year-around. That said, model simulations show that consistently ice-free winter conditions wont occur until atmospheric CO_2 levels reach around 1900 ppm [79], which is not expected until the 23rd century under even the strongest emission scenarios.

Method	Earliest ice-free	Consistently ice-free	Reference
Projections in terms of time			
CMIP3 models	2050 to >2100		[136]
selected & adjusted CMIP3 models	2018–2074#	2037	[54]
recalibrated CMIP3		2070*#	[58]
selected & adjusted CMIP5 models	2021–2043	2035	[100]
selected CMIP5		2041-2060	[13]
weighted CMIP5 models	2032–2046*	2039-2045*	[96]
CMIP5		2045–2070	[106]
weighted CMIP5		2062	[122]
CMIP5 large ensembles		2023–2079	[104]
selected CMIP5		2044–2067	[105]
constrained estimation of CMIP5		2056–2060	[137]
CESM1-LE	2032–2053	2040–2056	[15]
CESM2	2010–2042		[97]
CMIP6	<2014*to*¿2100*		[12]
selected CMIP6	2015–2052*		[12]
selected CMIP6		2035*	[16]
selected CMIP6		2043*	[17]
observationally-constrained CMIP6	2030s-2050s*	2040*#	[18]
statistical model using CMIP3 & observations		2066–2085	[94]
statistical model, CMIP6 & obs.		2036–2056*	[107]
statistical model		2039	[113]
Projections in terms of global warming			
recalibrated CMIP3 & obs. sea ice sensitivity		2.8 °C *#	[58]
observed sea ice sensitivity		1.8 °C #	[138]
sea ice sensitivity & MPI-ESM	1.5 °C *	2.0 °C *	[111]
bias corrected CESM1-LE	1.5 °C	2.5 °C #	[101]
constrained CanESM2	1.5 °C		[103]
CMIP6	0.9 °C – 3.2 °C *		[12]
selected CMIP6	1.3 °C – 2.9 °C *		[12]
observed sea ice sensitivity	1.5 °C *	<2 °C *	[112]

Table 1 Predictions of an ice-free Arctic from the literature, for the high emission scenario from each CMIP (SSP5-8.5 for CMIP6; RCP8.5 for CMIP5; A1B for CMIP3). "Earliest ice-free" refers to ice-free conditions diagnosed from unsmoothed timeseries, with a large impact of interannual variability. "Consistently ice-free" refers to ice-free conditions that exist in the ensemble mean or in the multi-year running mean or for several years in a row, and hence reflect when ice-free conditions occur due to the forced response. Results with a * indicate that the study used sea ice area, which leads to an earlier ice-free Arctic than using sea ice extent. Also note that some studies using sea ice area exclude areas of sea ice with less than 15% [17] while more commonly all sea ice present is included in the sea ice area calculation [12, 16, 18, 107, 111, 112]. Excluding areas with sea ice concentration below 15% leads to earlier ice-free years than when all sea ice is included in the sea ice area. Results marked with a # indicate years that were not explicitly stated in the respective study, and were instead read of figures or calculated relative to a different baseline; as such, years with # might differ by a few years from the values that could be obtained from the data underlying the cited publications. The first part of the table shows estimates in terms of time; the second part shows estimates in terms of global temperature anomalies to pre-industrial.

The length of the ice-free period matters, as the longer the Arctic is ice-free, the larger the impacts will be. Due to the seasonal cycle of the solar radiation north of the Arctic circle, ice-free conditions that begin earlier in the summer

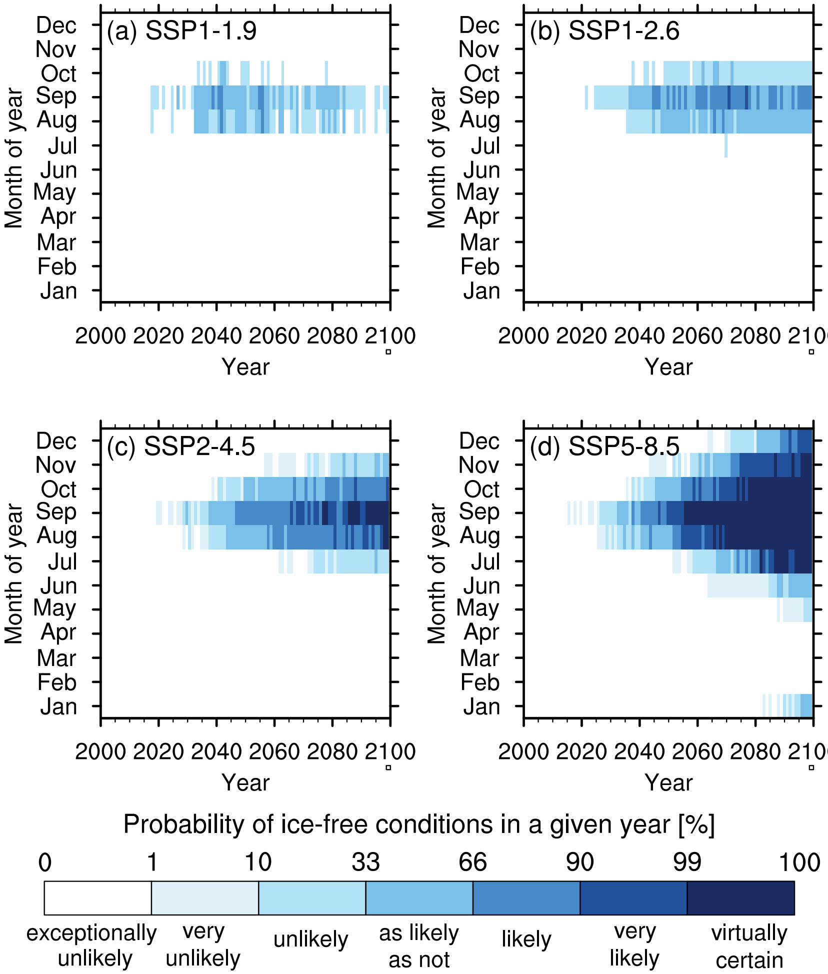

Fig. 4 Probability of ice-free conditions in all months of the year based on the selected CMIP6 models. a, The probability of ice-free conditions in a given year and month without any smoothing for selected CMIP6 models [12] forced with SSP1-1.9. The probability is given using the IPCC terms and percentage values. **b**, as in a, but for SSP1-2.6. **c**, as in a, but for SSP2-4.5. **d**, as in a, but for SSP5-8.5. There are large differences between scenarios in terms of how likely an ice-free Arctic is to occur in a given year's months, with the possibility of ice-free conditions limited to three months a year in SSP1-2.6 and SSP1-1.9 but extending to 5 months under SSP2-4.5 and 9 months under SSP5-8.5.

lead to more solar radiation uptake by the ocean and a stronger surface albedo feedback [49] as well as a larger impact on ocean productivity. Furthermore, the increased heat uptake by the ocean due to larger early open water areas delays the fall freeze up [139], leading to the extension of the ice-free season into the late fall [1, 101, 112].

Looking at predictions beyond September, there is a possibility for first ice-free conditions in August even if warming is kept to 2 °C [101, 111] (even in

SSP1-1.9Fig. 4). As warming increases further, additional months can experience first ice-free conditions (Fig. 4), for example in July, August, September and October for more than 2.5 °C global warming [111], and for November for over 3.5 °C [101]. In the selected CMIP6 models analysed here, some models even show first ice-free conditions for December and January as well as for May and June during second half of the 21st century under the SSP5-8.5 scenario (Fig. 4), when the CMIP6 multi-model warming is over 3.5 °C [134].

Consistently ice-free conditions in August could occur for 2.5 °C [111] to 3 °C of warming [101], similar to what is found here for the selected CMIP6 models with "likely" ice-free conditions in August after mid century under SSP2-4.5 (Fig. 4). Ice-free August's could be followed by consistently ice-free October's if warming reaches over 3.5 °C [101] or under SSP2-4.5 in the last decades of the 21st century in CMIP6 (Fig. 4). If warming exceeds 4 °C , likely ice-free conditions could also occur in Novembers [101], with ice-free conditions in July to October becoming very likely or virtually certain based on CMIP6 (Fig. 4). In terms of additional CO_2 emissions, predictions are that consistently ice-free conditions would begin to occur for July to October for an additional 1400 Gt CO_2 emissions and for November for around 3000 Gt CO_2 [1, 112]. In a few of the CMIP6 models, ice-free conditions even become likely in December at the end of the 21st century under SSP5-8.5 (Fig. 4), but not under the other emission scenarios.

In summary, there is a large scenario impact on how long the Arctic could be ice-free in a given year, with a possible range of 3 to 9 months of ice-free conditions possible by the end of the 21st century depending on the amount of future emissions.

4.3 Regional variations of ice-free Arctic conditions

Not many explicit predictions of regional ice-free conditions exist so far. In the predictions that exist [106, 140], the focus has been on consistently ice-free predictions. Comparing the results from CMIP5 and CMIP6 models, it is apparent that regional ice-free conditions occur on average earlier in CMIP6 models [140] than CMIP5 models [106], but with generally the same progression around the Arctic [140].

In both CMIP5 and CMIP6 models it has been found that the first entire seas to become consistently ice-free in September are predicted to be the on the Eurasian side of the Arctic, including the Kara Sea and the Laptev Sea [106, 140]. Ice-free conditions on the eastern side of the Arctic are predicted to be followed by ice-free conditions on the Pacific side, starting in the Chukchi Seas, followed by the East Siberian Sea and Beaufort Sea [106, 140]. The central Arctic is predicted to become ice-free last, if at all, depending on the scenario [106, 140, also see Fig. 5].

However, both CMIP5 [106] and CMIP6 [140] based regional ice-free predictions have uncertainties that are even larger than for the pan-Arctic. This larger uncertainty for regional predictions is due to the fact that they represent averages over smaller regions, which means that they are subject to larger internal variability as well as a smaller chance for compensating biases [106, 140]. Thus, given regional biases in climate simulations, the range of projected dates of regional ice-free conditions are quite dependent on which models are used as well as whether model selection was performed [106, 140].

In agreement with previous analysis, the spatial distribution of the timing of the first consistently ice-free conditions based on the selected CMIP6 models (Fig. 5) shows that the shelf seas become ice-free during the summer under all scenarios [140]. However, scenario differences have a big impact on when and if the central Arctic Ocean loses its sea ice cover in the CMIP6 ensemble mean in September by 2100 (Fig. 5) [140]. Furthermore, how much of the Arctic will not be ice-free during months beside September also has a strong scenario dependence. In particular, how much of the central Arctic will become ice-free in August and October is very dependent on the future emissions (Fig. 5), with implications for navigability of the transpolar sea route.

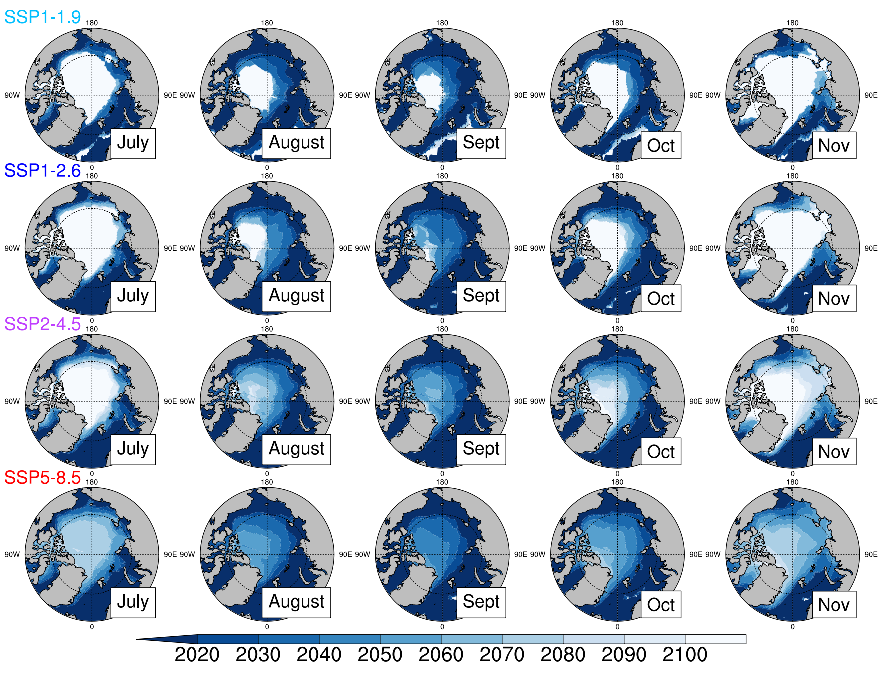

Fig. 5 Regional dates of first consistently ice-free conditions under different SSPs. **a**, regional consistently ice-free dates for July to November for SSP1-1.9, calculated as the first time the sea ice concentration in a grid box is below 15% in a given month in the average of the selected CMIP6 models[12] for each SSP. Bright white areas indicate regions that remain ice covered with more than 15% SIC in 2100 in the average of the selected CMIP6. Dark blue colors indicate areas that became ice-free before 2020 in the average of the selected CMIP6 or that never had ice cover. **b**, as in a, but for SSP1-2.6. **c**, as in a, but for SSP2-4.5. **d**, as in a, but for SSP5-8.5. Consistently ice-free dates occur last in the central Arctic Ocean. Regions that do not reach consistently ice-free conditions are largest in the SSP1-1.9 simulations, and are not expected to exist at all between July and November by 2090 in SSP5-8.5 simulations.

5 Summary and future perspectives

Based on various prediction approaches, an early first sea ice-free September might occur in the 2020s or 2030s, and is likely to occur by mid-century [12]. The possibility of early ice-free conditions in September is independent of emission scenario, as early ice-free conditions occur under all scenarios and warming levels assessed [12, 18, 101, 103], due to the short time to occurrence, so emission scenario differences are small [129, 130]. Due to the influence of internal variability, there only remains a small probability (<10%) that a first occurrence of an ice-free Arctic can still be avoided under the lowest warming scenarios where warming remains well under 2 °C [12, 101, 103]. However, it is important to highlight that greenhouse gas mitigation does affect ice-free conditions in the Arctic. Future levels of greenhouse gas emissions, and the associated degree of 21st century anthropogenic global warming will determine how often and for how long the Arctic will lose its sea ice cover. In particular under the low warming scenarios (SSP1-2.6), ice-free conditions could remain an exception rather than the new normal [101]. Furthermore, it has been repeatedly shown that sea ice recovers quickly when temperatures drop, for example in response to reductions in greenhouse gas concentrations [83–85]. Hence, Arctic sea ice does not have a tipping point, when such a tipping point is defined as an irreversible process or a system with multiple stable equilibria that the system can rapidly switch between. However, the absence of a tipping point for Arctic sea ice does not mean Arctic sea ice loss is not occurring rapidly or is not of importance. Changes in the Arctic sea ice have local as well as global implications, so the impacts of the loss of Arctic summer sea ice will not stay limited to the Arctic.

As the possible earliest date of an ice-free Arctic is approaching, its prediction and associated uncertainties need to be clearly communicated to set realistic expectations. Predictions of an ice-free Arctic should differentiate between predictions of "consistently ice-free conditions" or "likely" (>66%) ice-free conditions due to the forced response and predictions of the "earliest possible ice-free conditions", which can occur earlier over a decade earlier due to the influence of internal variability. A good way to provide both types of ice-free projections is to use cumulative probabilities (Fig. 3b, c, d) or the probability of ice-free conditions in a given year (Fig. 3e). Additionally, this clearly shows that ice-free predictions are always probabilistic, which is important to remember and communicate. Furthermore, it is also important to be aware that existing predictions of ice-free conditions (1) vary in whether they use a 1 million km^2 threshold in sea ice extent or area, with definitions using sea ice area leading to earlier ice-free conditions compared to those using sea ice extent [97] (Fig. 3a).

It also needs to be clearly communicated that currently published ice-free predictions focus on monthly averaged values. Ice-free conditions could occur even earlier when daily values are considered. In one model, the first day with a sea ice area of less than 1 million km^2 occurred on average 4 years before first monthly ice-free conditions, but with some ensemble members showing an earlier occurrence of daily ice-free conditions by over 10 years. Further work on predictions of daily ice-free conditions in the Arctic is needed to provide predictions of daily ice-free conditions and to assess whether models agree on the offset between daily and monthly ice-free conditions shown here based on one model.

Most predictions of ice-free conditions have been focused on pan-Arctic ice-free conditions. However, the transition to pan-Arctic ice free conditions occurs as regions progressively lose ice. Thus, strong regional impacts will take place prior to the Arctic reaching 1 million km^2 of sea ice. So far regional ice-free predictions have been rare [106, 140], and additional research is needed, in particular to develop methods to attempt to better constrain regional sea ice projections, which have even larger uncertainties than pan-Arctic ice-free projections [106, 140]. For example, it should be assessed how well existing model selection, recalibration, and observational constraints perform for sea ice projections in different regions of the Arctic. Based on the results of such analysis, new methods might need to be developed to better constrain regional sea ice projections from climate models, always accounting for the irreducible internal variability uncertainty.

Furthermore, as the first ice-free Arctic approaches, it is important to ensure that seasonal sea ice predictions have the skill needed to predict first ice-free conditions. Seasonal prediction of an early ice-free Arctic are likely to be particularly challenging, as sea ice predictions often perform least well when the decline in a given year is far from that expected from the long-term trend [141]. Seasonal prediction experiments initialized with climate model conditions several months prior to a simulated early ice-free state could provide useful insights on the predictability of these events. These prediction assessments of course have their limitations, in particular in terms of resolution and because climate models might lack processes that are important in the real world. Nonetheless, a test of seasonal prediction systems aimed at predictions of a first impending ice-free September could be very valuable to better understand which processes could lead to such events and to test existing seasonal prediction capabilities.

Another important issue to consider as an ice-free Arctic approaches is related as to when the Arctic sea ice community will consider having reached an ice-free Arctic. Deciding on this now is prudent, given that even for a given definition of ice-free, there is observational uncertainty in the satellite-derived sea ice area and sea ice extent products, as reflected by the difference between various observational sea ice concentration products (for example, Fig. 1d). As such, it is likely that the 1 million km^2 ice-free threshold will be crossed in some sea ice area or extent products but not others. Clarity on how this will be handled will facilitate communication around the occurrence of the first ice-free Arctic when it occurs.

To better constrain predictions of an ice-free Arctic, and of Arctic sea ice loss in general, dedicated intercomparisons of different model selection, recalibration and constraining methods would be very helpful to better understand the differences in their performance. Such a dedicated intercomparison is needed as currently too many parameters differ (models, ensemble members, emission scenarios, ice-free definitions) to identify the impact of an individual approach. Furthermore, defining a best practice for skillfully reducing the sea ice projection uncertainty would be very valuable for the community. In that process, further analysis should be performed to decide on the best metrics to base such methods on, so that they do not just reduce the projection uncertainty but in fact are likely to actually improve projection accuracy. Considering sea ice thickness [17] and ocean heat fluxes [16] as selection criteria should be part of that discussion. Additionally, biases in models should be used as an opportunity to better understand the real world [142]. For example, by studying what drives features not seen in models but present in observations, progress can be made on improving models.

Finally, there is an urgent need to gain a better understanding of both the impacts of an ice-free Arctic and the processes that could lead to an early ice-free Arctic. For the latter, research aimed at understanding the drivers of the internal variability ensemble spread of ice-free conditions are needed. Such research could provide answers as to what what is predictable and what is not predictable in regards to ice-free conditions, regionally and in the pan-Arctic mean. In terms of impacts of an ice-free Arctic, a more detailed understanding of the impacts of an ice-free Arctic, for example, on marine ecosystems, the global energy budget, wave height, and coastal erosion, are needed to better prepare for these impacts. Both kinds of research are timely given that ice-free conditions seem very likely to occur at least once by the middle of this century. In particular, understanding the nuances of the drivers and impacts of occasional daily ice-free conditions versus frequent monthly ice-free conditions versus ice-free conditions that occur for several months a year are needed to assess the true impact of what the transition of the Arctic sea ice cover into its new seasonal sea ice regime means in a warming world.

Glossary

- **sea ice area**: This term is used to refer to the total area of sea ice present, without any thresholds. It is calculated as follows: sea ice concentration times grid area summed over all grid boxes [40]. Note that sometimes, sea ice area is also calculated only for grid cells with at least 15% sea ice cover [17, 98, 143], but that is not how it is used here.
- **sea ice extent:** This is the term used to describe the area of all grid boxes that have at least 15% sea ice concentration. It is calculated as follows: for all grid boxes that have at least 15%, sea ice concentration is multiplied by the grid box area and then summed over all grid boxes with 15% or more sea ice concentration
- **internal variability**: The variability in the climate system due to the chaotic nature of the climate system

- **albedo**: Albedo is a term describing the fraction the incoming shortwave solar radiation that is reflected by a surface. It ranges between 0 and 1. Snow and ice have a high albedo, meaning a large percentage of the incoming shortwave solar radiation is reflected by the snow and ice. The ocean has a low albedo, meaning it absorbs a large percentage of the incoming shortwave solar radiation.
- **SSP**=Shared Socioeconomic pathway. A forcing scenario that is part of the ScenarioMIP of CMIP6.
- **sea ice sensitivity**: the change in sea ice area divided by the change in global or Arctic temperature or cumulative CO_2 emissions over the same time period.
- **fetch**: in oceanography, fetch refers to the horizontal distance over which wave generating winds blow
- **positive feedbacks**: Amplifying feedbacks in the climate system, enhancing an initial perturbation.
- **negative feedbacks**: Dampening feedbacks in the climate system, reducing an initial perturbation.
- **pan-Arctic**: used to refer to the whole Arctic.
- **CMIP6**= Climate Model Intercomparison project 6. There have been five different phases of CMIP so far, CMIP, CMIP2, CMIP3, CMIP5, and CMIP6.
- **tipping point**: An irreversible change in an environmental condition. Here used in regards to sea ice loss, so a tipping point would mean that decreasing the applied forcing does not reverse the sea ice loss seen under increasing forcing.
- **initial-value predictability**: refers to the predictability that arises from knowledge of an initial state.

Acknowledgments. We thanks Jakob Dörr for sharing the sea ice area data calculated for the SIMIP analysis [12] and Chris Wyburn-Powell for assistance with regridding the CMIP6 models for the spatial analysis. We also thank participants at the IARPC webinar on an ice-free Arctic for helpful discussions on this work, as well as three reviewers for constructive comments that helped us improve the manuscript. The NCAR Command Language (NCL) [144] was used for most of the analysis and the creation of figures, with the remaining analysis and plotting performed with python and IDL. We acknowledge the World Climate Research Programme, which, through its Working Group on Coupled Modelling, coordinated and promoted CMIP6. We thank the climate modeling groups for producing and making available their model output, the Earth System Grid Federation (ESGF) for archiving the data and providing access, and the multiple funding agencies who support CMIP6 and ESGF. We also acknowledge the US CLIVAR Working Group on Large Ensembles, the modeling centers that contributed to the CLIVAR Large Ensemble project, and the CESM2-LE project.

Declarations

- Funding: A. Jahn's contribution was supported by an Alexander von Humboldt Fellowship as well as by NSF CAREER award 1847398. M.M. Holland acknowledges support from NSF award 2138788 and 2040538. J.E. Kay's contribution was supported by NASA PREFIRE Award 849K995 and NSF award 2233420.
- Competing interests: The authors have no competing interests.
- Availability of data and materials: The CMIP6 sea ice area data is the same as analyzed in [12]. The underlying SIC data, also used for the spatial plot (Fig. 5), is available on the Earth System Grid Federation (ESGF, https://esgf-node.llnl.gov/search/cmip6/). The data for the CESM2-LE [135] is available at https://www.cesm.ucar.edu/projects/cvdp-le/data-repository. The data for the CLIVAR Large Ensemble Archive [145] is available at https://www.earthsystemgrid.org/dataset/ucar.cgd.ccsm4.CLIVAR_LE.html.
- Authors' contributions: A. Jahn decided on the overall scope of the article, wrote the majority of the article, and did all data analysis for the figures in the main article. M.M. Holland and J.E. Kay contributed to the writing of the manuscript, provided input on the article scope and figures, and edited the manuscript. M.M. Holland also performed data analysis for supplementary figures and created two of the figures.

References

[1] Stroeve, J. & Notz, D. Changing state of Arctic sea ice across all seasons. *Environmental Research Letters* **13** (10), 103001 (2018). https://doi.org/10.1088/1748-9326/aade56 .

[2] Cavalieri, D. J., Parkinson, C. L., Gloersen, P., Comiso, J. C. & Zwally, H. J. Deriving long-term time series of sea ice cover from satellite passive-microwave multisensor data sets. *J. Geophys. Res.* **104** (C7), 15803–15814 (1999). https://doi.org/10.1029/1999JC900081 .

[3] Kwok, R. & Rothrock, D. A. Decline in Arctic sea ice thickness from submarine and ICESat records: 1958–2008. *Geophys. Res. Lett.* **36** (2009). https://doi.org/10.1029/2009GL039035 .

[4] Kacimi, S. & Kwok, R. Arctic snow depth, ice thickness, and volume from icesat-2 and cryosat-2: 2018–2021. *Geophysical Research Letters* **49** (5), e2021GL097448 (2022). https://doi.org/10.1029/2021GL097448 .

[5] Meier, W., Fetterer, F., Windnagel, A. K. & Stewart, J. S. NOAA/NSIDC Climate Data Record of Passive Microwave Sea Ice Concentration, Version 4 (2021). URL https://nsidc.org/data/G02202/versions/4.

[6] England, M., Jahn, A. & Polvani, L. Nonuniform contribution of internal variability to recent Arctic sea ice loss. *J. Climate* **32** (13), 4039–4053 (2019). https://doi.org/10.1175/JCLI-D-18-0864.1 .

[7] Min, S., Zhang, X., Zwiers, F. & Agnew, T. Human influence on Arctic sea ice detectable from early 1990s onwards. *Geophys. Res. Lett.* **35** (2008). https://doi.org/10.1029/2008GL035725 .

[8] Kay, J. E., Holland, M. M. & Jahn, A. Inter-annual to multi-decadal Arctic sea ice extent trends in a warming world. *Geophys. Res. Let.* **38** (2011). https://doi.org/10.1029/2011GL048008 .

[9] Kirchmeier-Young, M. C., Zwiers, F. W. & Gillett, N. Attribution of extreme events in Arctic sea ice extent. *J. Climate* **30**, 553–571 (2017). https://doi.org/10.1175/JCLI-D-16-0412.1 .

[10] Parkinson, C. L. & Kellogg, W. Arctic sea ice decay simulated for a CO2-induced temperature rise. *Climatic Change* **2**, 149–162 (1979). https://doi.org/10.1007/BF00133221 .

[11] Rantanen, M. *et al.* The Arctic has warmed nearly four times faster than the globe since 1979. *Commun Earth Environ* **3** (168) (2022). https://doi.org/10.1038/s43247-022-00498-3 .

[12] SIMIP-Community. Arctic sea ice in CMIP6. *Geophysical Research Letters* **47** (10) (2020). https://doi.org/10.1029/2019GL086749 .

[13] Massonnet, F. *et al.* Constraining projections of summer Arctic sea ice. *The Cryosphere* **6** (6), 1383–1394 (2012). https://doi.org/10.5194/tc-6-1383-2012 .

[14] Notz, D. How well must climate models agree with observations? *Phil. Trans. R. Soc. A* **373** (2015). https://doi.org/10.1098/rsta.2014.0164 .

[15] Jahn, A., Kay, J., Holland, M. & Hall, D. How predictable is the timing of a summer ice-free Arctic? *Geophys. Res. Lett.* **43**, 9113–9120 (2016). https://doi.org/10.1002/2016GL070067 .

[16] Docquier, D. & Koenigk, T. Observation-based selection of climate models projects Arctic ice-free summers around 2035. *Commun Earth Environ* **2** (144) (2021). https://doi.org/10.1038/s43247-021-00214-7 .

[17] Zhou, X., Wang, B. & Huang, F. Evaluating sea ice thickness simulation is critical for projecting a summer ice-free Arctic Ocean. *Environmental Research Letters* **17** (11), 114033 (2022). URL https://dx.doi.org/10.1088/1748-9326/ac9d4d. https://doi.org/10.1088/1748-9326/ac9d4d .

[18] Kim, Y., Min, S., Gillett, N., Notz, D. & Malinina, E. Observationally-constrained projections of an ice-free Arctic even under a low emission scenario. *Nat Commun* **14** (2023). https://doi.org/10.1038/s41467-023-38511-8 .

[19] Topal, D. & Ding, Q. Atmospheric circulation-constrained model sensitivity recalibrates Arctic climate projections. *Nat. Clim. Chang.* (2023). https://doi.org/10.1038/s41558-023-01698-1 .

[20] Newton, R. *et al.* White Arctic vs. Blue Arctic: A case study of diverging stakeholder responses to environmental change. *Earth's Future* **4** (8), 396–405 (2016). https://doi.org/10.1002/2016EF000356 .

[21] Polyak, L. *et al.* History of sea ice in the Arctic. *Quaternary Science Reviews* **29**, 1757–1778 (2010). https://doi.org/10.1016/j.quascirev.2010.02.010 .

[22] Pistone, K., Eisenman, I. & Ramanathan, V. Observational determination of albedo decrease caused by vanishing Arctic sea ice. *Proceedings of the National Academy of Sciences* **111** (9), 3322–3326 (2014). https://doi.org/10.1073/pnas.1318201111 .

[23] Pistone, K., Eisenman, I. & Ramanathan, V. Radiative heating of an ice-free Arctic Ocean. *Geophysical Research Letters* **46** (13), 7474–7480 (2019) .

[24] Holland, M. & Bitz, C. Polar amplification of climate change in coupled models. *Climate Dynamics* **21**, 221–232 (2003). https://doi.org/10.1007/s00382-003-0332-6 .

[25] Screen, J. & Simmonds, I. The central role of diminishing sea ice in recent Arctic temperature amplification. *Nature* **464**, 1334–1337 (2010). https://doi.org/10.1038/nature09051 .

[26] Dai, A., D. Luo, D., Song, M. & Liu, J. Arctic amplification is caused by sea-ice loss under increasing co2. *Nat Commun* **10** (121) (2019). https://doi.org/10.1038/s41467-018-07954-9 .

[27] Jenkins, M. & Dai, A. The impact of sea-ice loss on Arctic climate feedbacks and their role for Arctic Amplification. *Geophysical Research Letters* **48** (15), e2021GL094599 (2021). https://doi.org/10.1029/2021GL094599 .

[28] Casas-Prat, M. & Wang, X. Sea ice retreat contributes to projected increases in extreme Arctic Ocean surface waves. *Geophysical Research Letters* **47** (15), e2020GL088100 (2020). https://doi.org/10.1029/2020GL088100 .

[29] Waseda, T. *et al.* Correlated increase of high ocean waves and winds in the ice-free waters of the Arctic Ocean. *Sci Rep* **8** (2018). https://doi.org/10.1038/s41598-018-22500-9 .

[30] Li, J., Ma, Y., Liu, Q., Zhang, W. & Guan, C. Growth of wave height with retreating ice cover in the Arctic. *Cold Regions Science and Technology* **164**, 102790 (2019). https://doi.org/10.1016/j.coldregions.2019.102790 .

[31] Overeem, I. *et al.* Sea ice loss enhances wave action at the Arctic coast. *Geophys. Res. Lett.* **38** (2011). https://doi.org/10.1029/2011GL048681 .

[32] Nielsen, D., Pieper, P. & Barkhordarian, A. Increase in Arctic coastal erosion and its sensitivity to warming in the twenty-first century. *Nat. Clim. Chang.* **12**, 263–270 (2022). https://doi.org/10.1038/s41558-022-01281-0 .

[33] Learmonth, J. A. *et al.* Potential effects of climate change on marine mammals. *Oceanography and Marine Biology* **44**, 431 (2006) .

[34] Regehr, E. V., Lunn, N. J., Amstrup, S. C. & Stirling, I. Effects of earlier sea-ice breakup on survival and population size of polar bears in western Hudson Bay. *Journal of Wildlife Management* **71**, 2673–2683 (2007) .

[35] Laidre, K. L. *et al.* Quantifying the sensitivity of Arctic marine mammals to climate-induced habitat change. *Ecological Applications* **18**, S97–S125 (2008) .

[36] Renaut, S., Devred, E. & Babin, M. Northward expansion and intensification of phytoplankton growth during the early ice-free season in Arctic. *Geophysical Research Letters* **45** (19), 10,590–10,598 (2018). https://doi.org/10.1029/2018GL078995 .

[37] Hollowed, A. B., Planque, B. & Loeng, H. Potential movement of fish and shellfish stocks from the sub-Arctic to the Arctic Ocean. *Fisheries Oceanography* **22** (5), 355–370 (2013). https://doi.org/10.1111/fog.12027 .

[38] Melia, N., Haines, K. & Hawkins, E. Sea ice decline and 21st century trans-Arctic shipping routes. *Geophysical Research Letters* **43** (18), 9720–9728 (2016). https://doi.org/10.1002/2016GL069315 .

[39] Schiermeier, Q. The great Arctic oil race begins. *Nature* **482**, 13–14 (2012). https://doi.org/10.1038/482013a .

[40] Dörr, J., Notz, D. & Kern, S. UHH sea ice area product (version 2019-fv0.01) (2021). URL https://www.cen.uni-hamburg.de/en/icdc/data/

cryosphere/uhh-sea-ice-area-product.html.

[41] Comiso, J. SSM/I concentrations using the Bootstrap Algorithm. *NASA Reference Publication 1380* (40 pg) (1995). URL Availablefrom:https://www.geobotany.uaf.edu/library/pubs/ComisoJC1995_nasa_1380_53.pdf .

[42] Cavalieri, D., Gloersen, P. & Campbell, W. Determination of sea ice parameters with the Nimbus 7 SMMR. *J. Geophys. Res.* **89**, 5355–5369 (1984). https://doi.org/10.1029/JD089iD04p05355 .

[43] Eyring, V. *et al.* Overview of the Coupled Model Intercomparison Project Phase 6 (CMIP6) experimental design and organization. *Geoscientific Model Development* **9** (5), 1937–1958 (2016). https://doi.org/10.5194/gmd-9-1937-2016 .

[44] Goosse, H. *et al.* Quantifying climate feedbacks in polar regions. *Nature Communications* **9** (2018). https://doi.org/10.1038/s41467-018-04173-0 .

[45] Pithan, F. & Mauritsen, T. Arctic amplification dominated by temperature feedbacks in contemporary climate models. *Nature Geosci* **7**, 181–184 (2014). https://doi.org/10.1038/ngeo2071 .

[46] Hahn, L. C., Armour, K. C., Zelinka, M. D., Bitz, C. M. & Donohoe, A. Contributions to polar amplification in CMIP5 and CMIP6 models. *Frontiers in Earth Science* **9** (2021). https://doi.org/10.3389/feart.2021.710036 .

[47] Bitz, C. M. & Roe, G. H. A mechanism for the high rate of sea ice thinning in the Arctic Ocean. *Journal of Climate* **17** (18), 3623 – 3632 (2004). https://doi.org/10.1175/1520-0442(2004)017⟨3623:AMFTHR⟩2.0.CO;2 .

[48] Massonnet, F. *et al.* Arctic sea-ice change tied to its mean state through thermodynamic processes. *Nature Clim Change* **8**, 599–603 (2018). https://doi.org/10.1038/s41558-018-0204-z .

[49] Holland, M. M. & Landrum, L. The emergence and transient nature of Arctic amplification in coupled climate models. *Frontiers in Earth Science* **9** (2021). https://doi.org/10.3389/feart.2021.719024 .

[50] Ding, Q. *et al.* Influence of high-latitude atmospheric circulation changes on summertime Arctic sea ice. *Nature Climate Change* **7**, 289–295 (2017). https://doi.org/10.1038/nclimate3241 .

[51] Roach, L. & Blanchard-Wrigglesworth, E. Observed winds crucial for Arctic sea ice loss. *Geophys. Res. Lett.* **49** (2022). https://doi.org/10.1029/2022GL097884 .

[52] Olonscheck, D., Mauritsen, T. & Notz, D. Arctic sea-ice variability is primarily driven by atmospheric temperature fluctuations. *Nat. Geosci.* **12**, 430–434 (2019). https://doi.org/10.1038/s41561-019-0363-1 .

[53] Polyakov, I. V. *et al.* Fluctuating Atlantic inflows modulate Arctic atlantification. *Science* **381** (6661), 972–979 (2023). https://doi.org/10.1126/science.adh5158 .

[54] Wang, M. & Overland, J. E. A sea ice free summer Arctic within 30 years? *Geophys. Res. Lett.* **36** (2009). https://doi.org/10.1029/2009GL037820 .

[55] Mueller, B., Gillett, N., Monahan, A., & Zwiers, F. Attribution of Arctic sea ice decline from 1953 to 2012 to influences from natural, greenhouse gas, and anthropogenic aerosol forcing. *J. Climate* **31** (19), 7771–7787 (2018). https://doi.org/10.1175/JCLI-D-17-0552.1 .

[56] Polvani, L. *et al.* Substantial twentieth-century Arctic warming caused by ozone-depleting substances. *Nature Climate Change* **10**, 130–133 (2020). https://doi.org/10.1038/s41558-019-0677-4 .

[57] England, M. R. & Polvani, L. M. The Montreal protocol is delaying the occurrence of the first ice-free Arctic summer. *Proceedings of the National Academy of Sciences* **120** (22), e2211432120 (2023). https://doi.org/10.1073/pnas.2211432120 .

[58] Mahlstein, I. & Knutti, R. September Arctic sea ice predicted to disappear near 2C global warming above present. *Geophys. Res. Lett.* **117** (2012). https://doi.org/10.1029/2011JD016709 .

[59] Stroeve, J. & Notz, D. Insights on past and future sea-ice evolution from combining observations and models. *Global and Planetary Change* **135**, 119–132 (2015). https://doi.org/10.1016/j.gloplacha.2015.10.011 .

[60] Notz, D. & Stroeve, J. Observed Arctic sea-ice loss directly follows anthropogenic CO_2 emission. *Science* (2016). https://doi.org/10.1126/science.aag2345 .

[61] Tarduno, J. A. *et al.* Evidence for extreme climatic warmth from late Cretaceous Arctic vertebrates. *Science* **282** (5397), 2241–2243 (1998). https://doi.org/10.1126/science.282.5397.2241 .

[62] Jenkyns, H., Forster, A., Schouten, S. & Damsté, J. S. S. High temperatures in the Late Cretaceous Arctic Ocean. *Nature* **432**, 888–892 (2004). https://doi.org/10.1038/nature03143 .

[63] Nathorst, A. G. Ueber die reste eines Brotfruchtbaums ARTOCARPUS DICKSONI n. sp., aus den cenomanen Kreideablagerungen Grönlands. *Kongl. Svenska Vetenskaps-Akad. Hand* **24**, 2–9 (1890) .

[64] Krylov, A. *et al.* A shift in heavy and clay mineral provenance indicates a middle Miocene onset of a perennial sea ice cover in the Arctic Ocean. *Paleoceanography* **23** (2008). https://doi.org/10.1029/2007PA001497 .

[65] Darby, D. Arctic perennial ice cover over the last 14 million years. *Paleoceanography* **23** (2008). https://doi.org/10.1029/2007PA001479 .

[66] Miller, G. *et al.* Temperature and precipitation history of the Arctic. *Quaternary Science Reviews* **29** (15), 1679–1715 (2010). https://doi.org/10.1016/j.quascirev.2010.03.001 .

[67] Tremblay, L. B., Schmidt, G. A., Pfirman, S., Newton, R. & DeRepentigny, P. Is ice-rafted sediment in a North Pole marine record evidence for perennial sea-ice cover? *Philosophical Transactions of the Royal Society A: Mathematical, Physical and Engineering Sciences* **373** (2052) (2015). https://doi.org/10.1098/rsta.2014.0168 .

[68] Stein, R. *et al.* Evidence for ice-free summers in the late Miocene central Arctic Ocean. *Nature Communications* **7** (1) (2016). https://doi.org/10.1038/ncomms11148 .

[69] Nøgaard-Pedersen, N., Mikkelsen, N. & Kristoffersen, Y. Arctic Ocean record of last two glacial-interglacial cycles off North Greenland/Ellesmere Island – Implications for glacial history. *Marine Geology* **244** (1), 93–108 (2007). https://doi.org/10.1016/j.margeo.2007.06.008 .

[70] Nørgaard-Pedersen, N., Mikkelsen, N., Lassen, S. J., Kristoffersen, Y. & Sheldon, E. Reduced sea ice concentrations in the Arctic Ocean during the last interglacial period revealed by sediment cores off northern Greenland. *Paleoceanography* **22** (1) (2007). https://doi.org/10.1029/2006PA001283 .

[71] Adler, R. E. *et al.* Sediment record from the western Arctic Ocean with an improved late Quaternary age resolution: HOTRAX core HLY0503-8JPC, Mendeleev Ridge. *Global and Planetary Change* **68** (1), 18–29 (2009). https://doi.org/10.1016/j.gloplacha.2009.03.026 .

[72] Sime, L. C., Sivankutty, R., Vallet-Malmierca, I., de Boer, A. M. & Sicard, M. Summer surface air temperature proxies point to near-sea-ice-free conditions in the Arctic at 127 ka. *Climate of the Past* **19** (4), 883–900 (2023). https://doi.org/10.5194/cp-19-883-2023 .

[73] Vermassen, F. *et al.* A seasonally ice-free Arctic Ocean during the Last Interglacial. *Nat. Geosci.* **16**, 723–729 (2023). https://doi.org/10.1038/s41561-023-01227-x .

[74] Lozhkin, A. V. & Anderson, P. M. The last interglaciation in northeast Siberia. *Quaternary Research* **43** (2), 147–158 (1995). https://doi.org/10.1006/qres.1995.1016 .

[75] de Vernal, A. *et al.* Natural variability of the Arctic Ocean sea ice during the present interglacial. *Proceedings of the National Academy of Sciences* **117** (42), 26069–26075 (2020). https://doi.org/10.1073/pnas.2008996117 .

[76] Jakobsson, M., Long, A., Ingoĺfsson, O., Kjær, K. H. & Spielhagen, R. F. New insights on Arctic Quaternary climate variability from palaeo-records and numerical modelling. *Quaternary Science Reviews* **29** (25), 3349–3358 (2010). https://doi.org/10.1016/j.quascirev.2010.08.016 .

[77] Pfirman, S., Fowler, C., Tremblay, B. & Newton, R. The last Arctic sea ice refuge. *The Circle* **4**, 6–8 (2009) .

[78] Newton, R., Pfirman, S., Tremblay, L. B. & DeRepentigny, P. Defining the "ice shed" of the Arctic Ocean's last ice area and its future evolution. *Earth's Future* **9** (9), e2021EF001988 (2021). https://doi.org/10.1029/2021EF001988 .

[79] Jahn, A. & Holland, M. M. Implications of Arctic sea ice changes for North Atlantic deep convection and the meridional overturning circulation in CCSM4-CMIP5 simulations. *Geophys. Res. Let.* **40** (6), 1206–1211 (2013). https://doi.org/10.1002/grl.50183 .

[80] Lenton, T. M. *et al.* Tipping elements in the earth's climate system. *Proceedings of the National Academy of Sciences* **105** (6), 1786–1793 (2008). https://doi.org/10.1073/pnas.0705414105 .

[81] North, G. R. Multiple solutions in energy balance climate models. *Global and Planetary Change* **2** (3), 225–235 (1990). https://doi.org/10.1016/0921-8181(90)90003-U .

[82] Eisenman, I. & Wettlaufer, J. S. Nonlinear threshold behavior during the loss of Arctic sea ice. *Proceedings of the National Academy of Sciences* **106** (1), 28–32 (2009). https://doi.org/10.1073/pnas.0806887106 .

[83] Tietsche, S., Notz, D., Jungclaus, J. H. & Marotzke, J. Recovery mechanisms of Arctic summer sea ice. *Geophysical Research Letters* **38** (2) (2011). https://doi.org/10.1029/2010GL045698 .

[84] Armour, K. C., Eisenman, I., Blanchard-Wrigglesworth, E., McCusker, K. E. & Bitz, C. M. The reversibility of sea ice loss in a state of the art climate model. *Geophys. Res. Lett.* **38** (2011). https://doi.org/10.1029/2011GL048739 .

[85] Li, C., Notz, D., Tietsche, S. & Marotzke, J. The transient versus the equilibrium response of sea ice to global warming. *J. Climate* **26**, 5624–5636 (2013). https://doi.org/10.1175/JCLI-D-12-00492.1 .

[86] Wagner, T. J. W. & Eisenman, I. How climate model complexity influences sea ice stability. *Journal of Climate* **28** (10), 3998 – 4014 (2015). https://doi.org/10.1175/JCLI-D-14-00654.1 .

[87] Holland, M. M., Bitz, C. M. & Tremblay, B. Future abrupt reductions in the summer Arctic sea ice. *Geophys. Res. Lett.* **33** (2006). https://doi.org/10.1029/2006GL028024 .

[88] Goosse, H., Arzel, O., Bitz, C. M., de Montety, A. & Vancoppenolle, M. Increased variability of the Arctic summer ice extent in a warmer climate. *Geophys. Res. Lett.* **36** (23) (2009). https://doi.org/10.1029/2009GL040546 .

[89] Mioduszewski, J. R., Vavrus, S., Wang, M., Holland, M. & Landrum, L. Past and future interannual variability in arctic sea ice in coupled climate models. *The Cryosphere* **13** (1), 113–124 (2019). https://doi.org/10.5194/tc-13-113-2019 .

[90] Auclair, G. & Tremblay, L. B. The role of ocean heat transport in rapid sea ice declines in the Community Earth System Model Large Ensemble. *J. Geophys. Res: Oceans* **123** (12), 8941–8957 (2018). https://doi.org/10.1029/2018JC014525 .

[91] Döscher, R. & Koenigk, T. Arctic rapid sea ice loss events in regional coupled climate scenario experiments. *Ocean Science* **9** (2), 217–248 (2013). https://doi.org/10.5194/os-9-217-2013 .

[92] Paquin, J.-P., Döscher, R., Sushama, L. & Koenigk, T. Causes and consequences of mid–21st-century rapid ice loss events simulated by the rossby centre regional atmosphere-ocean model. *Tellus A: Dynamic Meteorology and Oceanography* **65** (1) (2013). https://doi.org/10.3402/tellusa.v65i0.19110 .

[93] Vavrus, S., Holland, M. & Bailey, D. Changes in Arctic clouds during intervals of rapid sea ice loss. *Clim. Dyn.* **36** (7–8), 1475–1489 (2011). https://doi.org/10.1007/s00382-010-0816-0 .

[94] Boe, J., Hall, A. & Qu, X. September sea-ice cover in the Arctic Ocean projected to vanish by 2100. *Nature Geoscience* **2**, 341–343 (2009). https://doi.org/10.1038/ngeo467 .

[95] Pfirman, S., Haxby, W. F., Colony, R. & Rigor, I. Variability in the Arctic sea ice drift. *Geophys. Res. Lett.* **31** (2004). https://doi.org/10.1029/2004GL020063 .

[96] Snape, T. J. & Forster, P. M. Decline of Arctic sea ice: Evaluation and weighting of CMIP5 projections. *Journal of Geophysical Research: Atmospheres* **119** (2), 546–554 (2014). https://doi.org/10.1002/2013JD020593 .

[97] DeRepentigny, P., Jahn, A., Holland, M. M. & Smith, A. Arctic sea ice in two configurations of the CESM2 during the 20th and 21st centuries. *Journal of Geophysical Research: Oceans* **125** (9) (2020). https://doi.org/10.1029/2020JC016133 .

[98] Wang, B., Zhou, X., Ding, Q. & Liu, J. Increasing confidence in projecting the Arctic ice-free year with emergent constraints. *Environmental Research Letters* **16** (9) (2021). https://doi.org/10.1088/1748-9326/ac0b17 .

[99] Stocker, T. *et al.* (eds). *Technical Summary WG1*, book section TS, 33–115 (Cambridge University Press, Cambridge, United Kingdom and New York, NY, USA, 2013).

[100] Wang, M. & Overland, J. E. A sea ice free summer Arctic within 30 years: An update from cmip5 models. *Geophysical Research Letters* **39** (18) (2012). https://doi.org/10.1029/2012GL052868 .

[101] Jahn, A. Reduced probability of ice-free summers for 1.5C compared to 2C warming. *Nature Climate Change* **8** (5), 409–413 (2018). https://doi.org/10.1038/s41558-018-0127-8 .

[102] Screen, J. Arctic sea ice at 1.5 and 2 c. *Nature Climate Change* **8** (5), 362–363 (2018). https://doi.org/10.1038/s41558-018-0137-6 .

[103] Sigmond, M., Fyfe, J. C. & Swart, N. C. Ice-free Arctic projections under the Paris Agreement. *Nature Climate Change* **8** (5), 404–408 (2018). https://doi.org/10.1038/s41558-018-0124-y .

[104] Landrum, L. & Holland, M. Extremes become routine in an emerging new Arctic. *Nat. Clim. Chang.* **10**, 1108–1115 (2020). https://doi.org/10.1038/s41558-020-0892-z .

[105] Thackeray, C. & Hall, A. An emergent constraint on future Arctic sea-ice albedo feedback. *Nature Climate Change* **9**, 972–978 (2019). https://doi.org/10.1038/s41558-019-0619-1 .

[106] Laliberté, F., Howell, S. E. L. & Kushner, P. J. Regional variability of a projected sea ice-free Arctic during the summer months. *Geophysical Research Letters* **43** (1), 256–263 (2016). https://doi.org/10.1002/2015GL066855 .

[107] Bonan, D. B., Schneider, T., Eisenman, I. & Wills, R. C. J. Constraining the date of a seasonally ice-free Arctic using a simple model. *Geophysical Research Letters* **48** (18), e2021GL094309 (2021). https://doi.org/10.1029/2021GL094309 .

[108] Screen, J. A. & Williamson, D. Ice-free Arctic at 1.5C? *Nature Clim. Change* **7**, 230?231 (2017). https://doi.org/10.1038/nclimate3248 .

[109] Stroeve, J. C. *et al.* Trends in Arctic sea ice extent from CMIP5, CMIP3 and observations. *Geophys. Res. Lett.* **39** (2012). https://doi.org/10.1029/2012GL052676 .

[110] Ridley, J. K. & Blockley, E. W. Brief communication: Solar radiation management not as effective as co_2 mitigation for Arctic sea ice loss in hitting the 1.5 and 2c COP climate targets. *The Cryosphere* **12** (10), 3355–3360 (2018). https://doi.org/10.5194/tc-12-3355-2018 .

[111] Niederdrenk, A. L. & Notz, D. Arctic sea ice in a 1.5°c warmer world. *Geophysical Research Letters* **45** (4), 1963–1971 (2018). https://doi.org/10.1002/2017GL076159 .

[112] Notz, D. & Stroeve, J. The trajectory towards a seasonally ice-free Arctic ocean. *Curr Clim Change Rep* **4** (4), 407–416 (2018). https://doi.org/10.1007/s40641-018-0113-2 .

[113] Diebold, F. X. & Rudebusch, G. D. Probability assessments of an ice-free Arctic: Comparing statistical and climate model projections. *Journal of Econometrics* **231**, 520–534 (2022). https://doi.org/10.1016/j.jeconom.2020.12.007 .

[114] Hawkins, E. & Sutton, R. The potential to narrow uncertainty in regional climate predictions. *Bull. Amer. Meteor. Soc.* **90**, 1095–1107 (2009). https://doi.org/10.1175/2009BAMS2607.1 .

[115] Lorenz, E. N. Deterministic nonperiodic flow. *Journal of Atmospheric Sciences* **20** (2), 130 – 141 (1963). URL https://journals.ametsoc.org/view/journals/atsc/20/2/1520-0469_1963_020_0130_dnf_2_0_co_2.xml. https://doi.org/10.1175/1520-0469(1963)020⟨0130:DNF⟩2.0.CO;2 .

[116] Holland, M. & Hunke, E. A review of Arctic sea ice climate predictability in large-scale earth system models. *Oceanography* **35** (3-4), 20–27 (2022). https://doi.org/10.5670/oceanog.2022.113 .

[117] Screen, J. A. & Deser, C. Pacific ocean variability influences the time of emergence of a seasonally ice-free Arctic ocean. *Geophys. Res. Lett.* **46** (4), 2222–2231 (2019). https://doi.org/10.1029/2018GL081393 .

[118] Blanchard-Wrigglesworth, E., Bitz, C. M. & Holland, M. M. Influence of initial conditions and climate forcing on predicting Arctic sea ice. *Geophys. Res. Lett.* **38** (2011). https://doi.org/10.1029/2011GL048807 .

[119] Meier, W. N. & Stewart, J. S. Assessing uncertainties in sea ice extent climate indicators. *Environmental Research Letters* **14** (3), 035005 (2019). https://doi.org/10.1088/1748-9326/aaf52c .

[120] Swart, N. C., Fyfe, J. C., Hawkins, E., Kay, J. E. & Jahn, A. Influence of internal variability on Arctic sea-ice trends. *Nature Clim. Change* **5**, 86â89 (2015). https://doi.org/10.1038/nclimate2483 .

[121] Maslowski, W., Kinney, J. C., Higgins, M. & Roberts, A. The future of Arctic sea ice. *Annual Review of Earth and Planetary Sciences* **40**, 625–654 (2012). https://doi.org/10.1146/annurev-earth-042711-105345 .

[122] Senftleben, D., Lauer, A. & Karpechko, A. Constraining uncertainties in cmip5 projections of september Arctic sea ice extent with observations. *Journal of Climate* **33** (4), 1487 – 1503 (2020). https://doi.org/10.1175/JCLI-D-19-0075.1 .

[123] Liu J, W. H., Curry J. Impact of declining Arctic sea ice on winter snowfall. *Proc. Natl Acad. Sci.* **109** (2) (2012). https://doi.org/10.1073/pnas.1114910109 .

[124] Knutti, R. *et al.* A climate model projection weighting scheme accounting for performance and interdependence. *Geophysical Research Letters* **44** (4), 1909–1918 (2017). https://doi.org/10.1002/2016GL072012 .

[125] Aagaard, K. & Coachman, L. Toward an ice-free Arctic Ocean. *Eos, Transactions American Geophysical Union* **56** (7), 484–486 (1975). https://doi.org/10.1029/EO056i007p00484 .

[126] Khosravi, N. *et al.* The Arctic Ocean in CMIP6 models: Biases and projected changes in temperature and salinity. *Earth's Future* **10** (2), e2021EF002282 (2022). https://doi.org/10.1029/2021EF002282 .

[127] Muilwijk, M. *et al.* Divergence in climate model projections of future Arctic Atlantification. *Journal of Climate* **36** (6), 1727 – 1748 (2023). https://doi.org/10.1175/JCLI-D-22-0349.1 .

[128] Heuzè, C., Zanowski, H., Karam, S. & Muilwijk, M. The deep Arctic Ocean and Fram Strait in CMIP6 Models. *Journal of Climate* **36** (8), 2551 – 2584 (2023). https://doi.org/10.1175/JCLI-D-22-0194.1 .

[129] O'Neill, B. C. *et al.* The Scenario Model Intercomparison Project (ScenarioMIP) for CMIP6. *Geoscientific Model Development* **9** (9), 3461–3482 (2016). URL https://gmd.copernicus.org/articles/9/3461/2016/. https://doi.org/10.5194/gmd-9-3461-2016 .

[130] Bonan, D. B., Lehner, F. & Holland, M. M. Partitioning uncertainty in projections of Arctic sea ice. *Environmental Research Letters* **16** (4), 044002 (2021). https://doi.org/10.1088/1748-9326/abe0ec .

[131] Lindsay, R. W., Zhang, J., Schweiger, A., Steele, M. & Stern, H. Arctic sea ice retreat in 2007 follows thinning trend. *Journal of Climate* **22** (1), 165 – 176 (2009). https://doi.org/10.1175/2008JCLI2521.1 .

[132] Parkinson, C. L. & Comiso, J. C. On the 2012 record low Arctic sea ice cover: Combined impact of preconditioning and an August storm. *Geophys. Res. Lett.* **40**, 1356–1361 (2013). https://doi.org/10.1002/grl.50349 .

[133] Sanderson, B. *et al.* Community Climate Simulations to assess avoided impacts in 1.5C and 2C futures. *Earth Syst. Dynam.* **8**, 827–847 (2017). https://doi.org/10.5194/esd-8-827-2017 .

[134] Tebaldi, C. *et al.* Climate model projections from the scenario model intercomparison project (ScenarioMIP) of CMIP6. *Earth System Dynamics* **12** (1), 253–293 (2021). https://doi.org/10.5194/esd-12-253-2021 .

[135] Rodgers, K. B. *et al.* Ubiquity of human-induced changes in climate variability. *Earth System Dynamics* **12** (4), 1393–1411 (2021). https://doi.org/10.5194/esd-12-1393-2021 .

[136] Stroeve, J., Holland, M. M., Meier, W., Scambos, T. & Serreze, M. Arctic sea ice decline: Faster than forecast. *Geophys. Res. Lett.* **34** (2007). https://doi.org/10.1029/2007GL029703 .

[137] Liu, J., Song, M., Horton, R. M. & Hu, Y. Reducing spread in climate model projections of a September ice-free Arctic. *Proceedings of the National Academy of Sciences* **110** (31), 12571–12576 (2013). https://doi.org/10.1073/pnas.1219716110 .

[138] Rosenblum, E. & Eisenman, I. Faster Arctic sea ice retreat in CMIP5 than in CMIP3 due to volcanoes. *J Climate* **29**, 9179–9188 (2016). https://doi.org/10.1175/JCLI-D-16-0391.1 .

[139] Lebrun, M., Vancoppenolle, M., Madec, G. & Massonnet, F. Arctic sea-ice-free season projected to extend into autumn. *The Cryosphere* **13** (1), 79–96 (2019). https://doi.org/10.5194/tc-13-79-2019 .

[140] Arthun, M., Onarheim, I. H., Dörr, J. & Eldevik, T. The seasonal and regional transition to an ice-free Arctic. *Geophysical Research Letters* **48** (1), e2020GL090825 (2021). https://doi.org/10.1029/2020GL090825 .

[141] Hamilton, L. & Stroeve, J. 400 predictions: the SEARCH Sea Ice Outlook 2008–2015. *POLAR GEOGRAPHY,* **39** (4), 274–287 (2016). https://doi.org/10.1080/1088937X.2016.1234518 .

[142] Ding, Q. *et al.* Fingerprints of internal drivers of Arctic sea ice loss in observations and model simulations. *Nature Geoscience* **12**, 28–33 (2019). https://doi.org/10.1038/s41561-018-0256-8 .

[143] Fetterer, F., Knowles, K., Meier, W. & Savoie, M. Sea ice index. Digital media, updated daily, http://dx.doi.org/10.7265/N5QJ7F7W (2002).

[144] NCL. The NCAR Command Language (Version 6.6.2), Boulder, Colorado: UCAR/NCAR/CISL/TDD (2019).

[145] Deser, C. *et al.* Insights from earth system model initial-condition large ensembles and future prospects. *Nature Climate Change* (2020). https://doi.org/10.1038/s41558-020-0731-2 .

Supplementary Information for "Projections of an ice-free Arctic Ocean"

Alexandra Jahn†[1,2*], Marika M. Holland[3] and Jennifer E. Kay[1,4]

[1*]Department of Atmospheric and Oceanic Sciences, University of Colorado Boulder, Boulder,CO,USA.
[2]Institute for Arctic and Alpine Research, University of Colorado Boulder, Boulder,CO,USA.
[3]Climate & Global Dynamics Laboratory, National Center for Atmospheric Research, Boulder,CO,USA.
[4]Cooperative Institute for Research in Environmental Sciences, University of Colorado Boulder, Boulder,CO,USA.

†Corresponding author(s). E-mail(s): alexandra.jahn@colorado.edu;

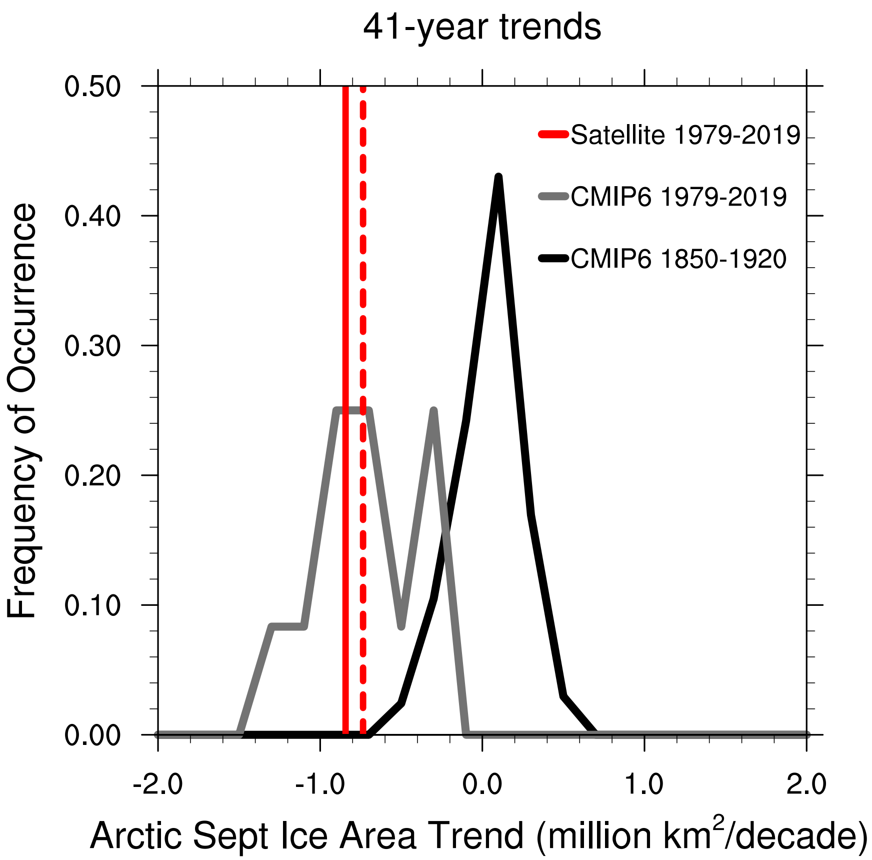

Supplementary Figure 1 Probability distribution of 41 year sea ice area trends for September, from the selected CMIP6 models for 1850-1920 (black) and 1979-2019 (grey) as well as from the 1979-2019 satellite-derived sea ice area data (red) [1], based on sea ice concentration data using the bootstrap [2] (solid red line) and NASA Team [3] (dashed red) algorithms. The shift in the two CMIP6 distributions show that that there has been a clear forced signal in the trends over 1979-2019 compared to 1850-1920, with more negative trends in 1979-2019. The observed trend over 1979-2019 does not fall within the CMIP6 ensemble spread for 1850-1920, but solidly within the CMIP6 ensemble spread for 1979-2019. Thus, this analysis supports that the observed sea ice loss has had a forced component.

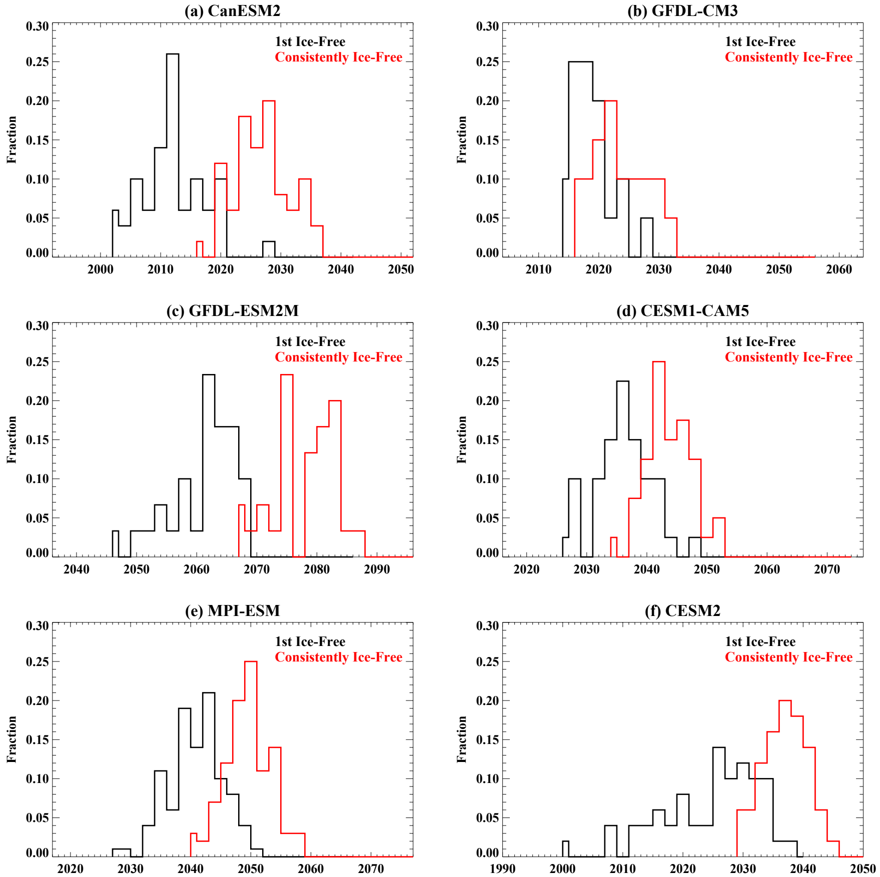

Supplementary Figure 2 Internal variability uncertainty for consistently versus first ice-free conditions in September. The comparison between the consistently ice-free ranges (red) and the first ice-free ranges (black) for different large ensembles **(a-f)** shows that that the internal variability uncertainty is generally reduced when going from the first ice-free conditions to consistently ice-free conditions, except for the GFDL-CM3, where the range increases (by 1 year). Furthermore, the distributions of consistently ice-free conditions are consistently shifted later compared to first ice-free conditions for all models. The consistently ice-free conditions are here calculated from 5yr running means. The models shown here are all large ensembles, primarily from CMIP5 models that are part of the CLIVAR Multi-Model Large ensemble archive [4], as well as from the last 50 members of the CMIP6 CESM2-LE [5].

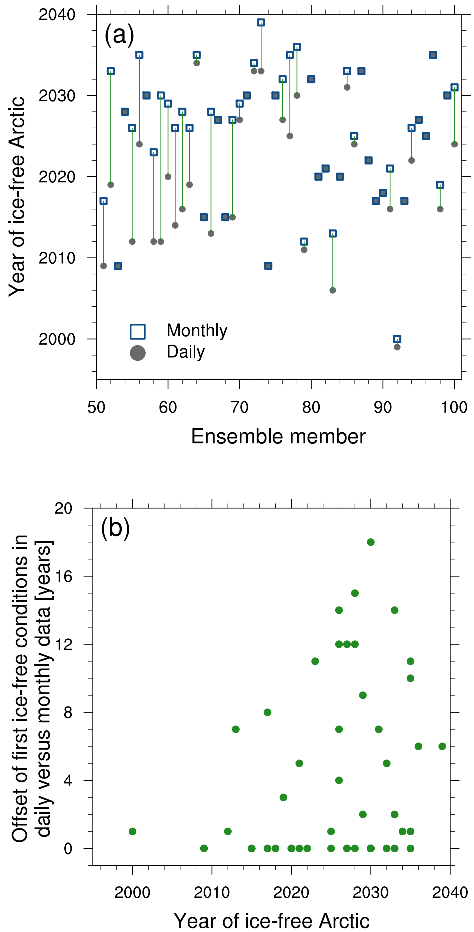

Supplementary Figure 3 Timing of a first ice-free Arctic in daily data versus monthly data. **a**, the first ice-free dates in individual ensemble members from members 51–100 of the CESM2-LE [5], showing the difference (green line) between ice-free conditions occurring in daily sea ice area data (grey) versus monthly mean sea ice area data (navy). **b**, The offset in ice-free dates between daily and monthly data from the same member shown in a (green), plotted over the first ice-free year from monthly data. This analysis shows that the difference between first daily and monthly ice free years for the same sea ice trajectory can range of 0–18 years, with the larger differences occurring for members that go ice-free late compared to the mean from members 51-100 of the CESM2-LE.

Model name	SSP1-1.9	SSP1-2.6	SSP2-4.5	SSP5-8.5
ACCESS-CM2	–	r1i1p1f1	r1i1p1f1	r1i1p1f1
ACCESS-ESM1-5	–	r1i1p1f1	r3i1p1f1	r1i1p1f1
CESM2-WACCM	–	r1i1p1f1	r1i1p1f1	r1i1p1f1
CNRM-ESM2-1	–	–	r1i1p1f2	–
CanESM5	r3i1p1f1	r7i1p1f1	r8i1p1f1	r7i1p1f1
EC-Earth3	–	r1i1p1f1	r1i1p1f1	r1i1p1f1
EC-Earth3-Veg	r2i1p1f1	r2i1p1f1	r8i1p1f1	r1i1p1f1
HadGEM3-GC31-LL	–	r1i1p1f3	r1i1p1f3	r2i1p1f3
IPSL-CM6A-LR	r1i1p1f1	r2i1p1f1	r5i1p1f1	r3i1p1f1
MIROC6	r1i1p1f1	r2i1p1f1	r1i1p1f1	r3i1p1f1
MRI-ESM2-0	r1i1p1f1	r1i1p1f1	r1i1p1f1	r1i1p1f1
NorESM2-LM	–	–	r1i1p1f1	–
AWI-CM-1-1-MR	–	r1i1p1f1	r1i1p1f1	r1i1p1f1
BCC-CSM2-MR	–	r1i1p1f1	r1i1p1f1	r1i1p1f1
CAMS-CSM1-0	r1i1p1f1	r1i1p1f1	r1i1p1f1	r1i1p1f1
CESM2	–	r2i1p1f1	r2i1p1f1	r2i1p1f1
CNRM-CM6-1	–	r1i1p1f2	r1i1p1f2	r1i1p1f2
CNRM-CM6-1-HR	–	–	r1i1p1f2	r1i1p1f2
FGOALS-f3-L	–	–	r1i1p1f1	–
FIO-ESM-2-0	–	r2i1p1f1	r2i1p1f1	r2i1p1f1
GFDL-CM4	–	–	r1i1p1f1	r1i1p1f1
GFDL-ESM4	r1i1p1f1	r1i1p1f1	r1i1p1f1	r1i1p1f1
HadGEM3-GC31-MM	–	r1i1p1f3	–	r2i1p1f3
INM-CM4-8	–	r1i1p1f1	r1i1p1f1	r1i1p1f1
INM-CM5-0	–	r1i1p1f1	r1i1p1f1	r1i1p1f1
MIROC-ES2L	r1i1p1f2	r1i1p1f2	r1i1p1f2	r1i1p1f2
MPI-ESM1-2-HR	–	r2i1p1f1	r1i1p1f1	r2i1p1f1
MPI-ESM1-2-LR	–	r2i1p1f1	r4i1p1f1	r4i1p1f1
NESM3	–	r1i1p1f2	r1i1p1f1	r1i1p1f1
UKESM1-0-LL	r1i1p1f2	r4i1p1f2	r3i1p1f2	r1i1p1f2

Supplementary Table 1 Listing of the CMIP6 ensemble members used. The CMIP6 data is the same as was used in [6] (see Supplementary Tables 2, 3, 4 for data citations). The ensemble member we used was chosen as the first of all available ensemble members that showed ice-free conditions in the monthly mean, as the focus of the analysis was on establishing the date of a possible early ice-free Arctic. The models above the horizontal line are the twelve selected models, based on [6]

Model name and experiment	data doi
ACCESS-CM2 historical	10.22033/ESGF/CMIP6.4271[7]
ACCESS-CM2 SSP1-2.6	10.22033/ESGF/CMIP6.4319[8]
ACCESS-CM2 SSP2-4.5	10.22033/ESGF/CMIP6.4322[9]
ACCESS-CM2 SSP5-8.5	10.22033/ESGF/CMIP6.4332[10]
ACCESS-ESM1-5 historical	10.22033/ESGF/CMIP6.4272[11]
ACCESS-ESM1-5 SSP1-2.6	10.22033/ESGF/CMIP6.4320[12]
ACCESS-ESM1-5 SSP2-4.5	10.22033/ESGF/CMIP6.4322[9]
ACCESS-ESM1-5 SSP5-8.5	10.22033/ESGF/CMIP6.4333[13]
CESM2-WACCM historcial	10.22033/ESGF/CMIP6.10071[14]
CESM2-WACCM SSP1-2.6	10.22033/ESGF/CMIP6.10100[15]
CESM2-WACCM SSP2-4.5	10.22033/ESGF/CMIP6.10101[16]
CNRM-ESM2-1 SSP5-8.5	10.22033/ESGF/CMIP6.10115[17]
CanESM5 historical	10.22033/ESGF/CMIP6.3610[18]
CanESM5 SSP1-1.9	10.22033/ESGF/CMIP6.3682[19]
CanESM5 SSP1-2.6	10.22033/ESGF/CMIP6.3683[20]
CanESM5 SSP2-4.5	10.22033/ESGF/CMIP6.3685[21]
CanESM5 SSP5-8.5	10.22033/ESGF/CMIP6.3696[22]
EC-Earth3 historical	10.22033/ESGF/CMIP6.4700[23]
EC-Earth3 SSP1-2.6	10.22033/ESGF/CMIP6.4874[24]
EC-Earth3 SSP2-4.5	10.22033/ESGF/CMIP6.4880[25]
EC-Earth3 SSP5-8.5	10.22033/ESGF/CMIP6.4912[26]
EC-Earth3-Veg historical	10.22033/ESGF/CMIP6.4706[27]
EC-Earth3-Veg SSP1-1.9	10.22033/ESGF/CMIP6.4872[28]
EC-Earth3-Veg SSP1-2.6	10.22033/ESGF/CMIP6.4876[29]
EC-Earth3-Veg SSP2-4.5	10.22033/ESGF/CMIP6.4882[30]
EC-Earth3-Veg SSP4-8.5	10.22033/ESGF/CMIP6.4914[31]
HadGEM3-GC31-LL historical	10.22033/ESGF/CMIP6.6109[32]
HadGEM3-GC31-LL SSP1-2.6	10.22033/ESGF/CMIP6.10849[33]
HadGEM3-GC31-LL SSP2-4.5	10.22033/ESGF/CMIP6.10851[34]
HadGEM3-GC31-LL SSP5-8.5	10.22033/ESGF/CMIP6.10901[35]
IPSL-CM6A-LR historical	10.22033/ESGF/CMIP6.5195[36]
IPSL-CM6A-LR SSP1-1.9	10.22033/ESGF/CMIP6.5261[37]
IPSL-CM6A-LR SSP1-2.6	10.22033/ESGF/CMIP6.5262[38]
IPSL-CM6A-LR SSP2-4.5	10.22033/ESGF/CMIP6.5264[39]
IPSL-CM6A-LR SSP5-8.5	10.22033/ESGF/CMIP6.5271[40]
MIROC6 historical	10.22033/ESGF/CMIP6.5603[41]
MIROC6 SSP1-1.9	10.22033/ESGF/CMIP6.5741[42]
MIROC6 SSP1-2.6	10.22033/ESGF/CMIP6.5743[43]
MIROC6 SSP2-4.5	10.22033/ESGF/CMIP6.5746[44]
MIROC6 SSP5-8.5	10.22033/ESGF/CMIP6.5771[45]
MRI-ESM2-0 historical	10.22033/ESGF/CMIP6.6842[46]
MRI-ESM2-0 SSP1-1.9	10.22033/ESGF/CMIP6.6908[47]
MRI-ESM2-0 SSP1-2.6	10.22033/ESGF/CMIP6.6909[48]
MRI-ESM2-0 SSP2-4.5	10.22033/ESGF/CMIP6.6910[49]
MRI-ESM2-0 SSP5-8.5	10.22033/ESGF/CMIP6.6929[50]
NorESM2-LM historical	10.22033/ESGF/CMIP6.8036[51]
NorESM2-LM SSP2-4.5	10.22033/ESGF/CMIP6.8253[52]

Supplementary Table 2 Data references for the selected CMIP6 models used

Model name and experiment	data doi
AWI-CM-1-1-MR historical	10.22033/ESGF/CMIP6.359 [53]
AWI-CM-1-1-MR SSP1-2.6	10.22033/ESGF/CMIP6.2796[54]
AWI-CM-1-1-MR SSP2-4.5	10.22033/ESGF/CMIP6.2800[55]
AWI-CM-1-1-MR SSP4-8.5	10.22033/ESGF/CMIP6.2817[56]
BCC-CSM2-MR historical	10.22033/ESGF/CMIP6.2948 [57]
BCC-CSM2-MR SSP1-2.6	10.22033/ESGF/CMIP6.3028[58]
BCC-CSM2-MR SSP2-4.5	10.22033/ESGF/CMIP6.3030 [59]
BCC-CSM2-MR SSP5-8.5	10.22033/ESGF/CMIP6.3050[60]
CAMS-CSM1-0 historical	10.22033/ESGF/CMIP6.9754[61]
CAMS-CSM1-0 SSP1-1.9	10.22033/ESGF/CMIP6.11045[62]
CAMS-CSM1-0 SSP1-2.6	10.22033/ESGF/CMIP6.11046[63]
CAMS-CSM1-0 SSP2-4.5	10.22033/ESGF/CMIP6.11047[64]
CAMS-CSM1-0 SSP5-8.5	10.22033/ESGF/CMIP6.11052 [65]
CESM2 historical	10.22033/ESGF/CMIP6.7627 [66]
CESM2 SSP1-2.6	10.22033/ESGF/CMIP6.7746[67]
CESM2 SSP2-4.5	10.22033/ESGF/CMIP6.7748[68]
CESM2 SSP5-8.5	10.22033/ESGF/CMIP6.7768 [69]
CNRM-CM6-1 historical	10.22033/ESGF/CMIP6.4066[70]
CNRM-CM6-1 SSP1-2.6	10.22033/ESGF/CMIP6.4184[71]
CNRM-CM6-1 SSP2-4.5	10.22033/ESGF/CMIP6.4189[72]
CNRM-CM6-1 SSP5-8.5	10.22033/ESGF/CMIP6.4224[73]
CNRM-CM6-1-HR historical	10.22033/ESGF/CMIP6.4067 [74]
CNRM-CM6-1-HR SSP2-4.5	10.22033/ESGF/CMIP6.4190[75]
CNRM-CM6-1-HR SSP5-8.5	10.22033/ESGF/CMIP6.4225[76]
FGOALS-f3-L historical	10.22033/ESGF/CMIP6.3355 [77]
FGOALS-f3-L SSP2-4.5	10.22033/ESGF/CMIP6.3468 [78]
FIO-ESM-2-0 historical	10.22033/ESGF/CMIP6.9199 [79]
FIO-ESM-2-0 SSP1-2.6	10.22033/ESGF/CMIP6.9208 [80]
FIO-ESM-2-0 SSP2-4.5	10.22033/ESGF/CMIP6.9209[81]
FIO-ESM-2-0 SSP5-8.5	10.22033/ESGF/CMIP6.9214[82]
GFDL-CM4 historical	10.22033/ESGF/CMIP6.8594[83]
GFDL-CM4 SSP2-4.5	10.22033/ESGF/CMIP6.9263[84]
GFDL-CM4 SSP5-8.5	10.22033/ESGF/CMIP6.9268[85]
GFDL-ESM4 historical	10.22033/ESGF/CMIP6.8597[86]
GFDL-ESM4 SSP1-1.9	10.22033/ESGF/CMIP6.8683[87]
GFDL-ESM4 SSP1-2.6	10.22033/ESGF/CMIP6.8684 [88]
GFDL-ESM4 SSP2-4.5	10.22033/ESGF/CMIP6.8686[89]
GFDL-ESM4 SSP5-8.5	10.22033/ESGF/CMIP6.8706[90]
HadGEM3-GC31-MM historical	10.22033/ESGF/CMIP6.6112 [91]
HadGEM3-GC31-MM SSP1-2.6	10.22033/ESGF/CMIP6.10850[92]
HadGEM3-GC31-MM SSP5-8.5	10.22033/ESGF/CMIP6.10902[93]
INM-CM4-8 historical	10.22033/ESGF/CMIP6.5069 [94]
INM-CM4-8 SSP1-2.6	10.22033/ESGF/CMIP6.12325[95]
INM-CM4-8 SSP2-4.5	10.22033/ESGF/CMIP6.12327[96]
INM-CM4-8 SSP5-8.5	10.22033/ESGF/CMIP6.12337[97]
INM-CM5-0 historical	10.22033/ESGF/CMIP6.5070 [98]
INM-CM5-0 SSP1-2.6	10.22033/ESGF/CMIP6.12326[99]
INM-CM5-0 SSP2-4.5	10.22033/ESGF/CMIP6.12328[100]
INM-CM5-0 SSP5-8.5	10.22033/ESGF/CMIP6.12338[101]
MIROC-ES2L historical	10.22033/ESGF/CMIP6.5602[102]
MIROC-ES2L SSP1-1.9	10.22033/ESGF/CMIP6.5740[103]
MIROC-ES2L SSP1-2.6	10.22033/ESGF/CMIP6.5742[104]
MIROC-ES2L SSP2-4.5	10.22033/ESGF/CMIP6.5745[105]
MIROC-ES2L SSP5-8.5	10.22033/ESGF/CMIP6.5770[106]

Supplementary Table 3 Data references for the additional CMIP6 models used

Model name and experiment	**data doi**
MPI-ESM1-2-HR historical	10.22033/ESGF/CMIP6.6594[107]
MPI-ESM1-2-HR SSP1-2.6	10.22033/ESGF/CMIP6.4397[108]
MPI-ESM1-2-HR SSP2-4.5	10.22033/ESGF/CMIP6.4398[109]
MPI-ESM1-2-HR SSP5-8.5	10.22033/ESGF/CMIP6.4403[110]
MPI-ESM1-2-LR historical	10.22033/ESGF/CMIP6.6595[111]
MPI-ESM1-2-LR SSP1-2.6	10.22033/ESGF/CMIP6.6690[112]
MPI-ESM1-2-LR SSP2-4.5	10.22033/ESGF/CMIP6.6693[113]
MPI-ESM1-2-LR SSP5-8.5	10.22033/ESGF/CMIP6.6705[114]
NESM3 historical	10.22033/ESGF/CMIP6.8769[115]
NESM3 SSp1-2.6	10.22033/ESGF/CMIP6.8780[116]
NESM3 SSP2-4.5	10.22033/ESGF/CMIP6.8781[117]
NESM3 SSP5-8.5	10.22033/ESGF/CMIP6.8790[118]
UKESM1-0-LL historical	10.22033/ESGF/CMIP6.6113 [119]
UKESM1-0-LL SSP1-1.9	10.22033/ESGF/CMIP6.6329[120]
UKESM1-0-LL SSP1-2.6	10.22033/ESGF/CMIP6.6333 [121]
UKESM1-0-LL SSP2-4.5	10.22033/ESGF/CMIP6.6339 [122]
UKESM1-0-LL SSP5-8.5	10.22033/ESGF/CMIP6.6405 [123]

Supplementary Table 4 Continued from Supplementary Table 3: Data references for the additional CMIP6 models used

References

[1] Dörr, J., Notz, D. & Kern, S. UHH sea ice area product (version 2019-fv0.01) (2021). URL https://www.cen.uni-hamburg.de/en/icdc/data/cryosphere/uhh-sea-ice-area-product.html.

[2] Comiso, J. SSM/I concentrations using the Bootstrap Algorithm. *NASA Reference Publication 1380* (40 pg) (1995). URL Availablefrom:https://www.geobotany.uaf.edu/library/pubs/ComisoJC1995_nasa_1380_53.pdf .

[3] Cavalieri, D., Gloersen, P. & Campbell, W. Determination of sea ice parameters with the Nimbus 7 SMMR. *J. Geophys. Res.* **89**, 5355–5369 (1984). https://doi.org/10.1029/JD089iD04p05355 .

[4] Deser, C. *et al.* Insights from earth system model initial-condition large ensembles and future prospects. *Nature Climate Change* (2020). https://doi.org/10.1038/s41558-020-0731-2 .

[5] Rodgers, K. B. *et al.* Ubiquity of human-induced changes in climate variability. *Earth System Dynamics* **12** (4), 1393–1411 (2021). https://doi.org/10.5194/esd-12-1393-2021 .

[6] SIMIP-Community. Arctic sea ice in CMIP6. *Geophysical Research Letters* **47** (10) (2020). https://doi.org/10.1029/2019GL086749 .

[7] Dix, M. *et al.* CSIRO-ARCCSS ACCESS-CM2 model output prepared for CMIP6 CMIP historical (2019). URL https://doi.org/10.22033/ESGF/CMIP6.4271.

[8] Dix, M. *et al.* CSIRO-ARCCSS ACCESS-CM2 model output prepared for CMIP6 ScenarioMIP SSP126 (2019). URL https://doi.org/10.22033/ESGF/CMIP6.4319.

[9] Ziehn, T. *et al.* CSIRO ACCESS-ESM1.5 model output prepared for CMIP6 ScenarioMIP SSP245 (2019). URL https://doi.org/10.22033/ESGF/CMIP6.4322.

[10] Dix, M. *et al.* CSIRO-ARCCSS ACCESS-CM2 model output prepared for CMIP6 ScenarioMIP SSP585 (2019). URL https://doi.org/10.22033/ESGF/CMIP6.4332.

[11] Ziehn, T. *et al.* CSIRO ACCESS-ESM1.5 model output prepared for CMIP6 CMIP historical (2019). URL https://doi.org/10.22033/ESGF/CMIP6.4272.

[12] Ziehn, T. *et al.* CSIRO ACCESS-ESM1.5 model output prepared for CMIP6 ScenarioMIP SSP126 (2019). URL https://doi.org/10.22033/ESGF/CMIP6.4320.

[13] Ziehn, T. *et al.* CSIRO ACCESS-ESM1.5 model output prepared for CMIP6 ScenarioMIP SSP585 (2019). URL https://doi.org/10.22033/ESGF/CMIP6.4333.

[14] Danabasoglu, G. NCAR CESM2-WACCM model output prepared for CMIP6 CMIP historical (2019). URL https://doi.org/10.22033/ESGF/CMIP6.10071.

[15] Danabasoglu, G. NCAR CESM2-WACCM model output prepared for CMIP6 ScenarioMIP SSP126 (2019). URL https://doi.org/10.22033/ESGF/CMIP6.10100.

[16] Danabasoglu, G. NCAR CESM2-WACCM model output prepared for CMIP6 ScenarioMIP SSP245 (2019). URL https://doi.org/10.22033/ESGF/CMIP6.10101.

[17] Danabasoglu, G. NCAR CESM2-WACCM model output prepared for CMIP6 ScenarioMIP SSP585 (2019). URL https://doi.org/10.22033/ESGF/CMIP6.10115.

[18] Swart, N. C. *et al.* CCCma CanESM5 model output prepared for CMIP6 CMIP historical (2019). URL https://doi.org/10.22033/ESGF/CMIP6.3610.

[19] Swart, N. C. *et al.* CCCma CanESM5 model output prepared for CMIP6 ScenarioMIP SSP119 (2019). URL https://doi.org/10.22033/ESGF/CMIP6.3682.

[20] Swart, N. C. *et al.* CCCma CanESM5 model output prepared for CMIP6 ScenarioMIP SSP126 (2019). URL https://doi.org/10.22033/ESGF/CMIP6.3683.

[21] Swart, N. C. *et al.* CCCma CanESM5 model output prepared for CMIP6 ScenarioMIP SSP245 (2019). URL https://doi.org/10.22033/ESGF/CMIP6.3685.

[22] Swart, N. C. *et al.* CCCma CanESM5 model output prepared for CMIP6 ScenarioMIP SSP585 (2019). URL https://doi.org/10.22033/ESGF/CMIP6.3696.

[23] (EC-Earth), E.-E. C. EC-Earth-Consortium EC-Earth3 model output prepared for CMIP6 CMIP historical (2019). URL https://doi.org/10.22033/ESGF/CMIP6.4700.

[24] (EC-Earth), E.-E. C. EC-Earth-Consortium EC-Earth3 model output prepared for CMIP6 ScenarioMIP SSP126 (2019). URL https://doi.org/10.22033/ESGF/CMIP6.4874.

[25] (EC-Earth), E.-E. C. EC-Earth-Consortium EC-Earth3 model output prepared for CMIP6 ScenarioMIP SSP245 (2019). URL https://doi.org/10.22033/ESGF/CMIP6.4880.

[26] (EC-Earth), E.-E. C. EC-Earth-Consortium EC-Earth3 model output prepared for CMIP6 ScenarioMIP SSP585 (2019). URL https://doi.org/10.22033/ESGF/CMIP6.4912.

[27] (EC-Earth), E.-E. C. EC-Earth-Consortium EC-Earth3-Veg model output prepared for CMIP6 CMIP historical (2019). URL https://doi.org/10.22033/ESGF/CMIP6.4706.

[28] (EC-Earth), E.-E. C. EC-Earth-Consortium EC-Earth3-Veg model output prepared for CMIP6 ScenarioMIP SSP119 (2019). URL https://doi.org/10.22033/ESGF/CMIP6.4872.

[29] (EC-Earth), E.-E. C. EC-Earth-Consortium EC-Earth3-Veg model output prepared for CMIP6 ScenarioMIP SSP126 (2019). URL https://doi.org/10.22033/ESGF/CMIP6.4876.

[30] (EC-Earth), E.-E. C. EC-Earth-Consortium EC-Earth3-Veg model output prepared for CMIP6 ScenarioMIP SSP245 (2019). URL https://doi.org/10.22033/ESGF/CMIP6.4882.

[31] (EC-Earth), E.-E. C. EC-Earth-Consortium EC-Earth3-Veg model output prepared for CMIP6 ScenarioMIP SSP585 (2019). URL https://doi.org/10.22033/ESGF/CMIP6.4914.

[32] Ridley, J., Menary, M., Kuhlbrodt, T., Andrews, M. & Andrews, T. MOHC HadGEM3-GC31-LL model output prepared for CMIP6 CMIP historical (2019). URL https://doi.org/10.22033/ESGF/CMIP6.6109.

[33] Good, P. MOHC HadGEM3-GC31-LL model output prepared for CMIP6 ScenarioMIP SSP126 (2020). URL https://doi.org/10.22033/ESGF/CMIP6.10849.

[34] Good, P. MOHC HadGEM3-GC31-LL model output prepared for CMIP6 ScenarioMIP SSP245 (2019). URL https://doi.org/10.22033/ESGF/CMIP6.10851.

[35] Good, P. MOHC HadGEM3-GC31-LL model output prepared for CMIP6 ScenarioMIP SSP585 (2020). URL https://doi.org/10.22033/ESGF/CMIP6.10901.

[36] Boucher, O. *et al.* IPSL IPSL-CM6A-LR model output prepared for CMIP6 CMIP historical (2018). URL https://doi.org/10.22033/ESGF/CMIP6.5195.

[37] Boucher, O. *et al.* IPSL IPSL-CM6A-LR model output prepared for CMIP6 ScenarioMIP SSP119 (2019). URL https://doi.org/10.22033/ESGF/CMIP6.5261.

[38] Boucher, O. *et al.* IPSL IPSL-CM6A-LR model output prepared for CMIP6 ScenarioMIP SSP126 (2019). URL https://doi.org/10.22033/ESGF/CMIP6.5262.

[39] Boucher, O. *et al.* IPSL IPSL-CM6A-LR model output prepared for CMIP6 ScenarioMIP SSP245 (2019). URL https://doi.org/10.22033/ESGF/CMIP6.5264.

[40] Boucher, O. *et al.* IPSL IPSL-CM6A-LR model output prepared for CMIP6 ScenarioMIP SSP585 (2019). URL https://doi.org/10.22033/ESGF/CMIP6.5271.

[41] Tatebe, H. & Watanabe, M. MIROC MIROC6 model output prepared for CMIP6 CMIP historical (2018). URL https://doi.org/10.22033/ESGF/CMIP6.5603.

[42] Shiogama, H., Abe, M. & Tatebe, H. MIROC MIROC6 model output prepared for CMIP6 ScenarioMIP SSP119 (2019). URL https://doi.org/10.22033/ESGF/CMIP6.5741.

[43] Shiogama, H., Abe, M. & Tatebe, H. MIROC MIROC6 model output prepared for CMIP6 ScenarioMIP SSP126 (2019). URL https://doi.org/10.22033/ESGF/CMIP6.5743.

[44] Shiogama, H., Abe, M. & Tatebe, H. MIROC MIROC6 model output prepared for CMIP6 ScenarioMIP SSP245 (2019). URL https://doi.org/10.22033/ESGF/CMIP6.5746.

[45] Shiogama, H., Abe, M. & Tatebe, H. MIROC MIROC6 model output prepared for CMIP6 ScenarioMIP SSP585 (2019). URL https://doi.org/10.22033/ESGF/CMIP6.5771.

[46] Yukimoto, S. *et al.* MRI MRI-ESM2.0 model output prepared for CMIP6 CMIP historical (2019). URL https://doi.org/10.22033/ESGF/CMIP6.6842.

[47] Yukimoto, S. *et al.* MRI MRI-ESM2.0 model output prepared for CMIP6 ScenarioMIP SSP119 (2019). URL https://doi.org/10.22033/ESGF/CMIP6.6908.

[48] Yukimoto, S. *et al.* MRI MRI-ESM2.0 model output prepared for CMIP6 ScenarioMIP SSP126 (2019). URL https://doi.org/10.22033/ESGF/CMIP6.6909.

[49] Yukimoto, S. *et al.* MRI MRI-ESM2.0 model output prepared for CMIP6 ScenarioMIP SSP245 (2019). URL https://doi.org/10.22033/ESGF/CMIP6.6910.

[50] Yukimoto, S. *et al.* MRI MRI-ESM2.0 model output prepared for CMIP6 ScenarioMIP SSP585 (2019). URL https://doi.org/10.22033/ESGF/CMIP6.6929.

[51] Seland, y. *et al.* NCC NorESM2-LM model output prepared for CMIP6 CMIP historical (2019). URL https://doi.org/10.22033/ESGF/CMIP6.8036.

[52] Seland, y. *et al.* NCC NorESM2-LM model output prepared for CMIP6 ScenarioMIP SSP245 (2019). URL https://doi.org/10.22033/ESGF/CMIP6.8253.

[53] Semmler, T. *et al.* AWI AWI-CM1.1MR model output prepared for CMIP6 CMIP (2018). URL https://doi.org/10.22033/ESGF/CMIP6.359.

[54] Semmler, T. *et al.* AWI AWI-CM1.1MR model output prepared for CMIP6 ScenarioMIP SSP126 (2018). URL https://doi.org/10.22033/ESGF/CMIP6.2796.

[55] Semmler, T. *et al.* AWI AWI-CM1.1MR model output prepared for CMIP6 ScenarioMIP SSP245 (2018). URL https://doi.org/10.22033/ESGF/CMIP6.2800.

[56] Semmler, T. *et al.* AWI AWI-CM1.1MR model output prepared for CMIP6 ScenarioMIP SSP585 (2019). URL https://doi.org/10.22033/ESGF/CMIP6.2817.

[57] Wu, T. *et al.* BCC BCC-CSM2MR model output prepared for CMIP6 CMIP historical (2018). URL https://doi.org/10.22033/ESGF/CMIP6.2948.

[58] Xin, X. *et al.* BCC BCC-CSM2MR model output prepared for CMIP6 ScenarioMIP SSP126 (2019). URL https://doi.org/10.22033/ESGF/CMIP6.3028.

[59] Xin, X. *et al.* BCC BCC-CSM2MR model output prepared for CMIP6 ScenarioMIP SSP245 (2019). URL https://doi.org/10.22033/ESGF/CMIP6.3030.

[60] Xin, X. *et al.* BCC BCC-CSM2MR model output prepared for CMIP6 ScenarioMIP SSP585 (2019). URL https://doi.org/10.22033/ESGF/CMIP6.3050.

[61] Rong, X. CAMS CAMS_CSM1.0 model output prepared for CMIP6 CMIP historical (2019). URL https://doi.org/10.22033/ESGF/CMIP6.9754.

[62] Rong, X. CAMS CAMS-CSM1.0 model output prepared for CMIP6 ScenarioMIP SSP119 (2019). URL https://doi.org/10.22033/ESGF/CMIP6.11045.

[63] Rong, X. CAMS CAMS-CSM1.0 model output prepared for CMIP6 ScenarioMIP SSP126 (2019). URL https://doi.org/10.22033/ESGF/CMIP6.11046.

[64] Rong, X. CAMS CAMS-CSM1.0 model output prepared for CMIP6 ScenarioMIP SSP245 (2019). URL https://doi.org/10.22033/ESGF/CMIP6.11047.

[65] Rong, X. CAMS CAMS-CSM1.0 model output prepared for CMIP6 ScenarioMIP SSP585 (2019). URL https://doi.org/10.22033/ESGF/CMIP6.11052.

[66] Danabasoglu, G. NCAR CESM2 model output prepared for CMIP6 CMIP historical (2019). URL https://doi.org/10.22033/ESGF/CMIP6.7627.

[67] Danabasoglu, G. NCAR CESM2 model output prepared for CMIP6 ScenarioMIP SSP126 (2019). URL https://doi.org/10.22033/ESGF/CMIP6.7746.

[68] Danabasoglu, G. NCAR CESM2 model output prepared for CMIP6 ScenarioMIP SSP245 (2019). URL https://doi.org/10.22033/ESGF/CMIP6.7748.

[69] Danabasoglu, G. NCAR CESM2 model output prepared for CMIP6 ScenarioMIP SSP585 (2019). URL https://doi.org/10.22033/ESGF/CMIP6.7768.

[70] Voldoire, A. CMIP6 simulations of the CNRM-CERFACS based on CNRM-CM6-1 model for CMIP experiment historical (2018). URL https://doi.org/10.22033/ESGF/CMIP6.4066.

[71] Voldoire, A. CNRM-CERFACS CNRM-CM6-1 model output prepared for CMIP6 ScenarioMIP SSP126 (2019). URL https://doi.org/10.22033/ESGF/CMIP6.4184.

[72] Voldoire, A. CNRM-CERFACS CNRM-CM6-1 model output prepared for CMIP6 ScenarioMIP SSP245 (2019). URL https://doi.org/10.22033/ESGF/CMIP6.4189.

[73] Voldoire, A. CNRM-CERFACS CNRM-CM6-1 model output prepared for CMIP6 ScenarioMIP SSP585 (2019). URL https://doi.org/10.22033/ESGF/CMIP6.4224.

[74] Voldoire, A. CNRM-CERFACS CNRM-CM6-1-HR model output prepared for CMIP6 CMIP historical (2019). URL https://doi.org/10.22033/ESGF/CMIP6.4067.

[75] Voldoire, A. CNRM-CERFACS CNRM-CM6-1-HR model output prepared for CMIP6 ScenarioMIP SSP245 (2019). URL https://doi.org/10.22033/ESGF/CMIP6.4190.

[76] Voldoire, A. CNRM-CERFACS CNRM-CM6-1-HR model output prepared for CMIP6 ScenarioMIP SSP585 (2019). URL https://doi.org/10.22033/ESGF/CMIP6.4225.

[77] YU, Y. CAS FGOALS-f3-L model output prepared for CMIP6 CMIP historical (2019). URL https://doi.org/10.22033/ESGF/CMIP6.3355.

[78] YU, Y. CAS FGOALS-f3-L model output prepared for CMIP6 ScenarioMIP SSP245 (2019). URL https://doi.org/10.22033/ESGF/CMIP6.3468.

[79] Song, Z. *et al.* FIO-QLNM FIO-ESM2.0 model output prepared for CMIP6 CMIP historical (2019). URL https://doi.org/10.22033/ESGF/CMIP6.9199.

[80] Song, Z. *et al.* FIO-QLNM FIO-ESM2.0 model output prepared for CMIP6 ScenarioMIP SSP126 (2019). URL https://doi.org/10.22033/ESGF/CMIP6.9208.

[81] Song, Z. *et al.* FIO-QLNM FIO-ESM2.0 model output prepared for CMIP6 ScenarioMIP SSP245 (2019). URL https://doi.org/10.22033/ESGF/CMIP6.9209.

[82] Song, Z. *et al.* FIO-QLNM FIO-ESM2.0 model output prepared for CMIP6 ScenarioMIP SSP585 (2019). URL https://doi.org/10.22033/ESGF/CMIP6.9214.

[83] Guo, H. *et al.* NOAA-GFDL GFDL-CM4 model output historical (2018). URL https://doi.org/10.22033/ESGF/CMIP6.8594.

[84] Guo, H. *et al.* NOAA-GFDL GFDL-CM4 model output prepared for CMIP6 ScenarioMIP SSP245 (2018). URL https://doi.org/10.22033/ESGF/CMIP6.9263.

[85] Guo, H. *et al.* NOAA-GFDL GFDL-CM4 model output prepared for CMIP6 ScenarioMIP SSP585 (2018). URL https://doi.org/10.22033/ESGF/CMIP6.9268.

[86] Krasting, J. P. *et al.* NOAA-GFDL GFDL-ESM4 model output prepared for CMIP6 CMIP historical (2018). URL https://doi.org/10.22033/ESGF/CMIP6.8597.

[87] John, J. G. *et al.* NOAA-GFDL GFDL-ESM4 model output prepared for CMIP6 ScenarioMIP SSP119 (2018). URL https://doi.org/10.22033/ESGF/CMIP6.8683.

[88] John, J. G. *et al.* NOAA-GFDL GFDL-ESM4 model output prepared for CMIP6 ScenarioMIP SSP126 (2018). URL https://doi.org/10.22033/ESGF/CMIP6.8684.

[89] John, J. G. *et al.* NOAA-GFDL GFDL-ESM4 model output prepared for CMIP6 ScenarioMIP SSP245 (2018). URL https://doi.org/10.22033/ESGF/CMIP6.8686.

[90] John, J. G. *et al.* NOAA-GFDL GFDL-ESM4 model output prepared for CMIP6 ScenarioMIP SSP585 (2018). URL https://doi.org/10.22033/ESGF/CMIP6.8706.

[91] Ridley, J., Menary, M., Kuhlbrodt, T., Andrews, M. & Andrews, T. MOHC HadGEM3-GC31-MM model output prepared for CMIP6 CMIP historical (2019). URL https://doi.org/10.22033/ESGF/CMIP6.6112.

[92] Jackson, L. MOHC HadGEM3-GC31-MM model output prepared for CMIP6 ScenarioMIP SSP126 (2020). URL https://doi.org/10.22033/ESGF/CMIP6.10850.

[93] Jackson, L. MOHC HadGEM3-GC31-MM model output prepared for CMIP6 ScenarioMIP SSP585 (2020). URL https://doi.org/10.22033/ESGF/CMIP6.10902.

[94] Volodin, E. *et al.* INM INM-CM4-8 model output prepared for CMIP6 CMIP historical (2019). URL https://doi.org/10.22033/ESGF/CMIP6.5069.

[95] Volodin, E. *et al.* INM INM-CM4-8 model output prepared for CMIP6 ScenarioMIP SSP126 (2019). URL https://doi.org/10.22033/ESGF/CMIP6.12325.

[96] Volodin, E. *et al.* INM INM-CM4-8 model output prepared for CMIP6 ScenarioMIP SSP245 (2019). URL https://doi.org/10.22033/ESGF/CMIP6.12327.

[97] Volodin, E. *et al.* INM INM-CM4-8 model output prepared for CMIP6 ScenarioMIP SSP585 (2019). URL https://doi.org/10.22033/ESGF/CMIP6.12337.

[98] Volodin, E. *et al.* INM INM-CM5-0 model output prepared for CMIP6 CMIP historical (2019). URL https://doi.org/10.22033/ESGF/CMIP6.5070.

[99] Volodin, E. *et al.* INM INM-CM5-0 model output prepared for CMIP6 ScenarioMIP SSP126 (2019). URL https://doi.org/10.22033/ESGF/CMIP6.12326.

[100] Volodin, E. *et al.* INM INM-CM5-0 model output prepared for CMIP6 ScenarioMIP SSP245 (2019). URL https://doi.org/10.22033/ESGF/CMIP6.12328.

[101] Volodin, E. *et al.* INM INM-CM5-0 model output prepared for CMIP6 ScenarioMIP SSP585 (2019). URL https://doi.org/10.22033/ESGF/CMIP6.12338.

[102] Hajima, T. *et al.* MIROC MIROC-ES2L model output prepared for CMIP6 CMIP historical (2019). URL https://doi.org/10.22033/ESGF/CMIP6.5602.

[103] Tachiiri, K. *et al.* MIROC MIROC-ES2L model output prepared for CMIP6 ScenarioMIP SSP119 (2019). URL https://doi.org/10.22033/ESGF/CMIP6.5740.

[104] Tachiiri, K. *et al.* MIROC MIROC-ES2L model output prepared for CMIP6 ScenarioMIP SSP126 (2019). URL https://doi.org/10.22033/ESGF/CMIP6.5742.

[105] Tachiiri, K. *et al.* MIROC MIROC-ES2L model output prepared for CMIP6 ScenarioMIP SSP245 (2019). URL https://doi.org/10.22033/ESGF/CMIP6.5745.

[106] Tachiiri, K. *et al.* MIROC MIROC-ES2L model output prepared for CMIP6 ScenarioMIP SSP585 (2019). URL https://doi.org/10.22033/ESGF/CMIP6.5770.

[107] Jungclaus, J. *et al.* MPI-M MPI-ESM1.2-HR model output prepared for CMIP6 CMIP historical (2019). URL https://doi.org/10.22033/ESGF/CMIP6.6594.

[108] Schupfner, M. *et al.* DKRZ MPI-ESM1.2-HR model output prepared for CMIP6 ScenarioMIP SSP126 (2019). URL https://doi.org/10.22033/ESGF/CMIP6.4397.

[109] Schupfner, M. *et al.* DKRZ MPI-ESM1.2-HR model output prepared for CMIP6 ScenarioMIP SSP245 (2019). URL https://doi.org/10.22033/ESGF/CMIP6.4398.

[110] Schupfner, M. *et al.* DKRZ MPI-ESM1.2-HR model output prepared for CMIP6 ScenarioMIP SSP585 (2019). URL https://doi.org/10.22033/ESGF/CMIP6.4403.

[111] Wieners, K.-H. *et al.* MPI-M MPI-ESM1.2-LR model output prepared for CMIP6 CMIP historical (2019). URL https://doi.org/10.22033/ESGF/CMIP6.6595.

[112] Wieners, K.-H. *et al.* MPI-M MPI-ESM1.2-LR model output prepared for CMIP6 ScenarioMIP SSP126 (2019). URL https://doi.org/10.22033/ESGF/CMIP6.6690.

[113] Wieners, K.-H. *et al.* MPI-M MPI-ESM1.2-LR model output prepared for CMIP6 ScenarioMIP SSP245 (2019). URL https://doi.org/10.22033/ESGF/CMIP6.6693.

[114] Wieners, K.-H. *et al.* MPI-M MPI-ESM1.2-LR model output prepared for CMIP6 ScenarioMIP SSP585 (2019). URL https://doi.org/10.22033/ESGF/CMIP6.6705.

[115] Cao, J. & Wang, B. NUIST NESMv3 model output prepared for CMIP6 CMIP historical (2019). URL https://doi.org/10.22033/ESGF/CMIP6.8769.

[116] Cao, J. NUIST NESMv3 model output prepared for CMIP6 ScenarioMIP SSP126 (2019). URL https://doi.org/10.22033/ESGF/CMIP6.8780.

[117] Cao, J. NUIST NESMv3 model output prepared for CMIP6 ScenarioMIP SSP245 (2019). URL https://doi.org/10.22033/ESGF/CMIP6.8781.

[118] Cao, J. NUIST NESMv3 model output prepared for CMIP6 ScenarioMIP SSP585 (2019). URL https://doi.org/10.22033/ESGF/CMIP6.8790.

[119] Tang, Y. *et al.* MOHC UKESM1.0-LL model output prepared for CMIP6 CMIP historical (2019). URL https://doi.org/10.22033/ESGF/CMIP6.6113.

[120] Good, P. *et al.* MOHC UKESM1.0-LL model output prepared for CMIP6 ScenarioMIP SSP119 (2019). URL https://doi.org/10.22033/ESGF/CMIP6.6329.

[121] Good, P. *et al.* MOHC UKESM1.0-LL model output prepared for CMIP6 ScenarioMIP SSP126 (2019). URL https://doi.org/10.22033/ESGF/CMIP6.6333.

[122] Good, P. *et al.* MOHC UKESM1.0-LL model output prepared for CMIP6 ScenarioMIP SSP245 (2019). URL https://doi.org/10.22033/ESGF/CMIP6.6339.

[123] Good, P. *et al.* MOHC UKESM1.0-LL model output prepared for CMIP6 ScenarioMIP SSP585 (2019). URL https://doi.org/10.22033/ESGF/CMIP6.6405.